Journal of Hydrology 563 (2018) 319–335

Contents lists available at ScienceDirect

Journal of Hydrology

journal homepage: www.elsevier.com/locate/jhydrol

Research papers

Spatial resolutions in areal rainfall estimation and their impact on hydrological simulations of a lowland catchment

Wilco Terink[a,d,*], Hidde Leijnse[b], Gé van den Eertwegh[c], Remko Uijlenhoet[d]

[a] Regional Council, 200 Tuam Street, PO Box 345, Christchurch, New Zealand
[b] Royal Netherlands Meteorological Institute (KNMI), Utrechtseweg 297, 3731 GA De Bilt, The Netherlands
[c] KnowH2O, Watertorenweg 12, 6571 CB Berg en Dal, The Netherlands
[d] Hydrology and Quantitative Water Management Group, Wageningen University, Droevendaalsesteeg 4, 6708 PB Wageningen, The Netherlands

ARTICLE INFO

This manuscript was handled by Marco borga, Editor-in-Chief, with the assistance of Francesco Marra, Associate Editor

Keywords:
X-band radar
SPHY
Spatial resolutions
Hydrological simulations
Uncertainty
Hupsel Brook catchment

ABSTRACT

Many studies suggest that high-density rain gauge networks are required to capture the rainfall heterogeneities necessary to accurately describe the components of the hydrological cycle. However, equipping and maintaining a high-density rain gauge network will also involve high costs. Although many studies provided useful insights on the required accuracy of rainfall estimates to accurately describe the components of the hydrological cycle, most of these studies focused on streamflow simulations, large river basins or urban environments. The objective of this study is therefore to evaluate the impact of uncertainties in areal rainfall, estimated at several spatial resolutions, on hydrological simulations of a small ~6.5 km^2 rural lowland catchment. The approach followed in this study is to force a calibrated spatially-distributed hydrological model (SPHY) with rainfall retrieved from an X-band radar and various synthetic rainfall products, calculated using bootstrap samples of a varying number of radar pixels, treated as virtual rain gauge locations within the catchment. This enables us to determine the most appropriate resolution of rainfall data to accurately describe the hydrology of a small rural lowland catchment. We found that the use of one rain gauge to estimate the catchment's areal rainfall may lead to a potential error of more than six times the average hourly rainfall. This may lead to uncertainties in simulated discharge that approach 60% of the average hourly discharge. More than 40 rain gauges are required to reduce the potential error in areal rainfall estimation to values < 0.1 mm h^{-1}. The associated uncertainty in discharge simulations is 20% if 10 rain gauges are used, and 10% if 40 rain gauges are used. The simulation of soil moisture contents and evapotranspiration rates are hardly affected by the number of rain gauges used to estimate the areal rainfall, which is due to the high saturated hydraulic conductivities of the top-soil. At least 12 gauges per km^2 are required to capture the spatial rainfall variation that is present in radar rainfall estimates. Analysis of an individual 18-h rainfall event revealed that the uncertainty in peak areal rainfall estimated using one rain gauge may range between −100% and 600%. The associated uncertainty in simulated discharge for this event ranges between −67 and 233%. With 25 rain gauges the uncertainty in simulated discharge is still in the range of −17 to 33%.

1. Introduction

It is well-known that rainfall is a highly heterogeneous process covering an extensive range of scales in time and space (Marani, 2005; Nicótina, 2008). Despite the fact that accurate estimates of rainfall in terms of location and intensity are crucial for operational water management, as well as for the hydrological research community (Van de Beek et al., 2010), hydrologists have traditionally put more effort in the development of evermore sophisticated rainfall-runoff modeling approaches than in the development of improved techniques for the measurement and prediction of the space–time variability of rainfall (Berne et al., 2005). However, during the last few years substantial effort has been put in modeling high-resolution rainfall in both space and time (Paschalis et al., 2013; Nerini et al., 2017; Peleg et al., 2017).

Traditionally, the rain gauge has been the most common instrument to measure rainfall (Sohn et al., 2010; Van de Beek et al., 2010; Van de Beek et al., 2012). A disadvantage of a rain gauge is that it only provides point measurements and therefore lacks information on the spatial variability (Van de Beek et al., 2010), unless used in a network of rain gauges with a sufficient density. Lebel et al. (1987) showed that if rainfall measurements are based on ground measurements only, their accuracy depends on the spatial variability of the rainfall process and

* Corresponding author at: Regional Council, 200 Tuam Street, PO Box 345, Christchurch, New Zealand.
E-mail addresses: wilco.terink@ecan.govt.nz (W. Terink), hidde.leijnse@knmi.nl (H. Leijnse), eertwegh@knowh2o.nl (G. van den Eertwegh), remko.uijlenhoet@wur.nl (R. Uijlenhoet).

https://doi.org/10.1016/j.jhydrol.2018.05.045
Received 3 January 2018; Received in revised form 18 May 2018; Accepted 19 May 2018
Available online 22 May 2018

the density of the rain gauge network. For short timescales (up to 15 min) and regions that are characterized by frequent low rainfall rates, the spatial rainfall correlations are likely to be corrupted by measurement uncertainties (Villarini et al., 2008). Peleg et al. (2013) found that at least three rain stations are needed to adequately represent the rainfall on a typical radar pixel scale. Berne et al. (2005) concluded that the uncertainty in hourly discharge simulations associated with the sampling uncertainty of the mean areal rainfall estimated over a ~1600 km^2 catchment from 10 rain gauges was ± 25%, being of the same order of magnitude as that associated with the model variables describing the initial state of the model. Faurès et al. (1995) concluded that the use of a single rain gauge can lead to large uncertainties in runoff estimations for a small-scale (4.4 ha) semi-arid catchment, dominated by convective rainfall. This suggests that high-density rain gauge networks are required to capture the rainfall heterogeneities necessary to accurately describe the components of the hydrological cycle (Lobligeois et al., 2014). However, equipping and maintaining a high-density rain gauge network will also involve high costs (Pardo-Igúzquiza, 1998). In order to be more cost-effective, water managers would therefore benefit from information indicating the number of rain gauges, their spatial distribution, and measuring interval required to accurately describe the hydrological processes in their management area.

Other techniques to measure rainfall include the use of weather radar (Berne et al., 2005; Berne et al., 2004; Van de Beek et al., 2012), disdrometers (Joss and Waldvogel, 1969) and microwave links (Leijnse et al., 2007a,b; Overeem et al., 2013). All these instruments have their pros and cons when it comes to measuring rainfall. Compared to the use of a single rain gauge, weather radar is capable of capturing the spatial variability of rainfall over larger areas (Van de Beek et al., 2012; Van de Beek et al., 2010), although it is well-known that data obtained from weather radars are affected by multiple sources of error (Hazenberg et al., 2011; Villarini and Krajewski, 2010). Weather radar and rain gauges are complementary to each other and are therefore often combined to generate bias-corrected weather radar images (Hazenberg et al., 2011; Rabiei and Haberlandt, 2015). The potential of weather radar retrieved rainfall for hydrological applications has been investigated in several studies (e.g. Berne et al., 2005; Van de Beek et al., 2010; Ochoa-Rodriguez et al., 2015; Paschalis et al., 2014). Berne et al. (2005) investigated the potential of a C-band doppler weather radar for hydrological applications in the Ourthe catchment (~1600 km^2), Belgium. Forcing the lumped HBV model with the radar-estimated mean areal rainfall, they found a significant underestimation with respect to the observed discharge. Hazenberg et al. (2011) corrected the same C-band doppler weather radar for errors related to attenuation, ground clutter, anomalous propagation, the vertical profile of reflectivity, and advection, and demonstrated the potential of applying weather radar information as input to the HBV model, without using any rain gauge information. Van de Beek et al. (2010) evaluated the performance of high-resolution X-band radar for rainfall measurement in The Netherlands, and found that X-band radar is able to measure the space–time variation of rainfall at high resolution, far greater than what can be achieved by rain gauge networks.

It is clear that a key question to be answered is: “what is the accuracy of rainfall measurements that is required to accurately describe the components of the hydrological cycle” (Bell et al., 2000; Nicótina, 2008)?. According to the studies above this issue is dominated by the spatial resolution of the rainfall product used. Others (Brauer et al., 2016; Krajewski et al., 1991; Wilson et al., 1979), however, have concluded that the temporal rather than the spatial variability plays a primary role in the hydrologic response, with Brauer et al. (2016) and Krajewski et al. (1991) focusing on small catchments (<7.5 km^2). Huza et al. (2014) highlights the strong relation between the occurrence of flash floods and initial soil moisture conditions. Other studies (Van de Beek et al., 2012; Berne et al., 2004; Berndtsson and Niemczynowicz, 1988; Ogden et al., 1997; Ochoa-Rodriguez et al., 2015; Rafieeinasab et al., 2015; Yang et al., 2016) found that rainfall measurements with high spatial and temporal resolutions are especially required for urban environments with fast response times. Nicótina (2008) analyzed the influence of rainfall variability on the hydrologic response as a function of characteristic spatial scales of rainfall events, water transport processes in hillslopes and the channel network, runoff generation mechanisms, and basin scale, and concluded that the spatial variability of rainfall does not significantly influence the flood response for basin areas up to 3,500 km^2. Bell et al. (2000) evaluated the sensitivity of a lumped and a distributed rainfall-runoff model to rainfall estimates at a variety of resolutions, focusing on both stratiform and convective events. They found that a distributed model using rain gauge data as input is sensitive to the location of rain gauges within the catchment, and therefore to the spatial variability of rainfall over the catchment, with a stronger sensitivity for convective rainfall. However, they did not relate the required resolution of rainfall data to the spatial resolution of the rainfall-runoff models used.

Although these studies provided useful insights on the accuracy of rainfall measurements that is required at different spatial and temporal resolutions to be able to accurately describe the components of the hydrological cycle, most of them focused on streamflow only. Besides streamflow, other components of the hydrological cycle, such as soil moisture content and evapotranspiration are relevant as well for e.g. agriculture. The majority of studies above focused on river basins in the order of 100–1,000 km^2 (Lebel et al., 1987; Nicótina, 2008; Bell et al., 2000; Berne et al., 2005), while another substantial number of studies (Van de Beek et al., 2012; Berne et al., 2004; Berndtsson and Niemczynowicz, 1988; Ogden et al., 1997) focused on urban environments with fast response times. We feel that the spatial resolution required for areal rainfall estimation to accurately describe the hydrological processes in small (<10 km^2) rural lowland (slightly sloping and freely draining (Brauer et al., 2014)) catchments requires additional attention. The objective of this study is therefore to evaluate the impact of areal rainfall, estimated at several spatial resolutions, on hydrological simulations of a small rural lowland catchment.

The approach followed in this study is to force a spatially-distributed hydrological model with rainfall retrieved from an X-band radar (Van de Beek et al., 2010; Sassi et al., 2014) and various synthetic rainfall products, calculated using bootstrap samples of a varying number of radar pixels, treated as virtual rain gauge locations within the catchment. This enables us to determine the most appropriate resolution of rainfall data to accurately describe the hydrology of a small rural lowland catchment. The Royal Netherlands Meteorological Institute (KNMI) operates two C-band Doppler radars (Overeem et al., 2009), each providing rainfall images at a 1-km spatial and 5-min temporal resolutions. Given the course resolution of the C-band radar data (1 km) with respect to the catchment size (6.5 km^2), we have chosen to use X-band radar data from a different location rather than C-band radar data at the location of the catchment because of their higher space time resolution available. Also, disaggregating C-band radar to higher resolutions means we need to make assumptions about the small-scale rainfall variability, which are very uncertain and are not needed in our case with X-band radar. Another advantage of using X-band radar is that it allows for the detection of convective rainfall events. The used X-band radar provides a higher spatial (120 m range; 1.875 degrees in azimuth) and temporal (16 s) resolution than the C-band radar operated by the KNMI. The Hupsel Brook catchment (Section 2.1) was selected as case-study catchment for this study. This catchment was also used by Brauer et al. (2016) to analyze the effect of differences between rainfall measurement techniques on groundwater and discharge simulations, and by Brauer et al. (2011) to study the hydrological response of this catchment for an extraordinary rainfall event. During 24 h on the 26th of August 2010, nearly 160 mm of rain was recorded by the meteorological station in the Hupsel Brook catchment, which is operated by the KNMI. This extraordinary rainfall event, with an estimated return period of more than 1000 years, caused

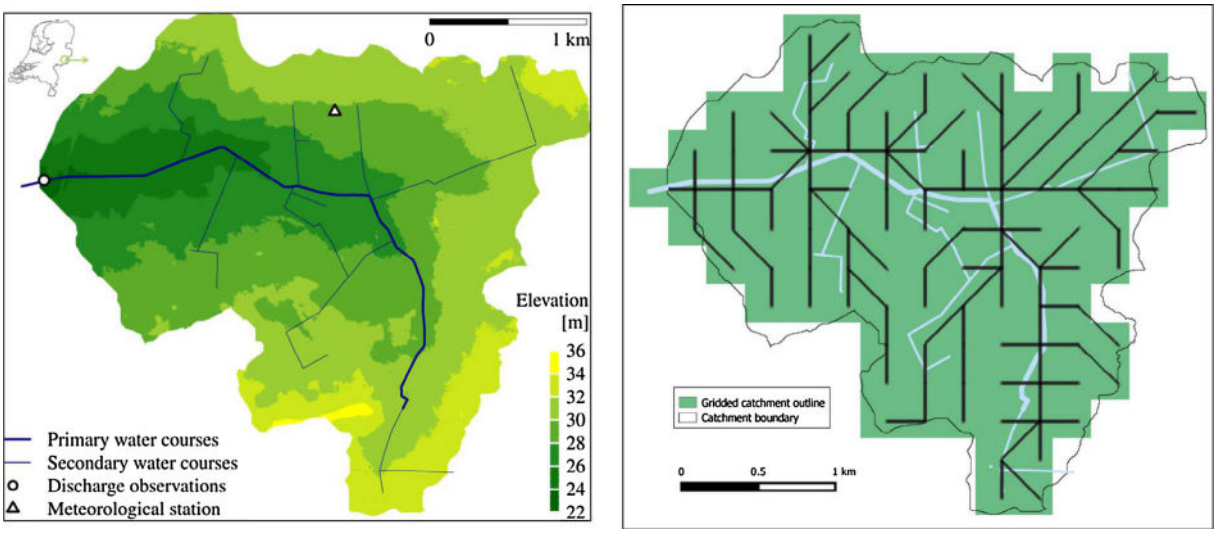

Fig. 1. Left: the Hupsel Brook catchment in the east of the Netherlands including its discharge and meteorological stations (tertiary channels and drains are not shown). Right: the gridded model outline of the Hupsel Brook catchment at a 250 m spatial resolution. Each grid cell has a drainage direction (derived from the Digital Elevation Model (DEM)), which is represented by the black lines, and is therefore part of the channel network. Delineating channel networks in lowland catchments based on a DEM is often a constraint, which explains why the delineated channel network is not a perfect match with reality.

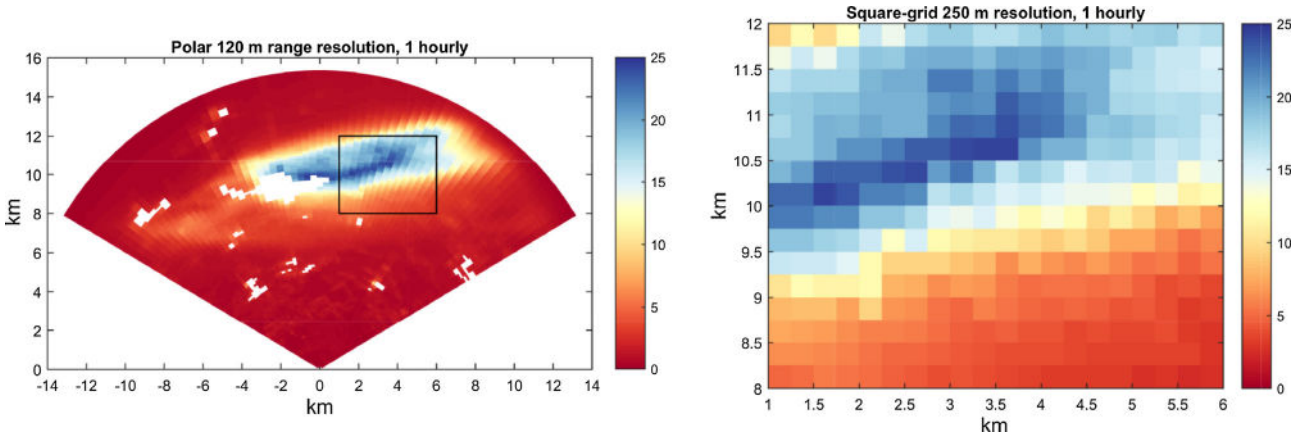

Fig. 2. Left: Example of an aggregated hourly X-band radar image with rain intensity in mm h^{-1} and range resolution of 120 m. Right: Example of an aggregated hourly X-band radar image with rain intensity in mm h^{-1} at a 250 m resolution square grid. The Hupsel Brook catchment rainfall data is extracted from the black rectangle. White areas represent radar clutter. (For interpretation of the references to colour in this figure legend, the reader is referred to the web version of this article.)

inundation of several plots in the area. Within seven hours the discharge increased from 5×10^{-2} to almost 4.5 $m^3 s^{-1}$ (Brauer et al., 2011). The study by Brauer et al. (2011) underlines the importance of having high-quality rainfall data, which justifies the context of the current study; if high quality rainfall data would have been available, then timely measures could have been taken to reduce the risk of flooding and minimize damage. Additionally, such extraordinary rainfall events help us to better understand the hydrological processes involved.

This paper is organized as follows: Section 2 describes the study area and the X-band radar data used to derive the synthetic rainfall products. Section 3 describes the methodology used to remove residual clutter, obtain the synthetic rainfall products, and the set-up of the spatially distributed hydrological model. The results are presented in Section 4 and discussed in Section 5. The conclusions are given in Section 6.

2. Data

2.1. Hupsel Brook Catchment

The Hupsel Brook catchment is a small (6.5 km^2) lowland catchment located in the east of the Netherlands (Fig. 1). The Hupsel Brook is a naturally drained catchment, but since 1960 drain pipes and culverts have been constructed (Warmerdam, 1979). These drains have been constructed in 50% of the plots and cause, together with the dense network of ditches, a fast discharge response when the catchment is close to saturation (van der Velde et al., 2009). Land use in the catchment consists of grass (59%), agriculture (33%), forest (3%), and urban areas (5%) (Brauer et al., 2011). Elevation within the catchment varies from 22 m.a.s.l. in the west to 35 m.a.s.l. in the southeast. The mean

Table 1
Optimized SPHY model parameters obtained through calibration for the period 2001–2009. $K_{satfact}$ is not a model parameter, but a factor used to optimize the spatial K_{sat} values for the root- and subzone layer.

Acronym	Description	Calibrated value	Units
δ_{gw}	groundwater recharge delay time	160	h
kx	flow recession coefficient	0.75	–
$GW_{satfrac}$	saturated fraction of groundwater layer	0.10	$m^3\ m^{-3}$
$K_{satfact}$	K_{sat} factor	1.5	–

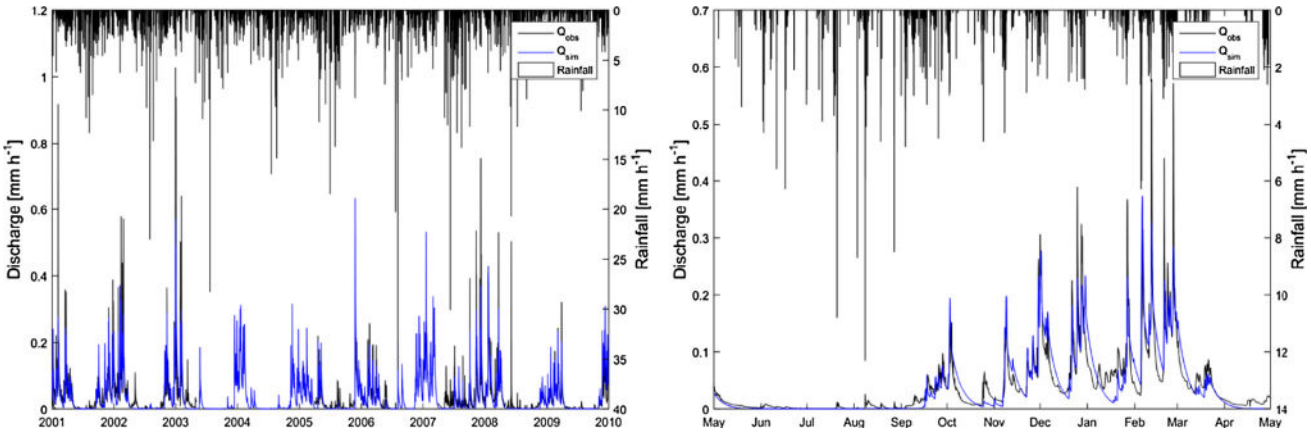

Fig. 3. Left: observed (Q_{obs}) and SPHY simulated discharge (Q_{sim}) for the calibration period 2001–2009. Right: idem, but for the hydrological year May 2001–April 2002.

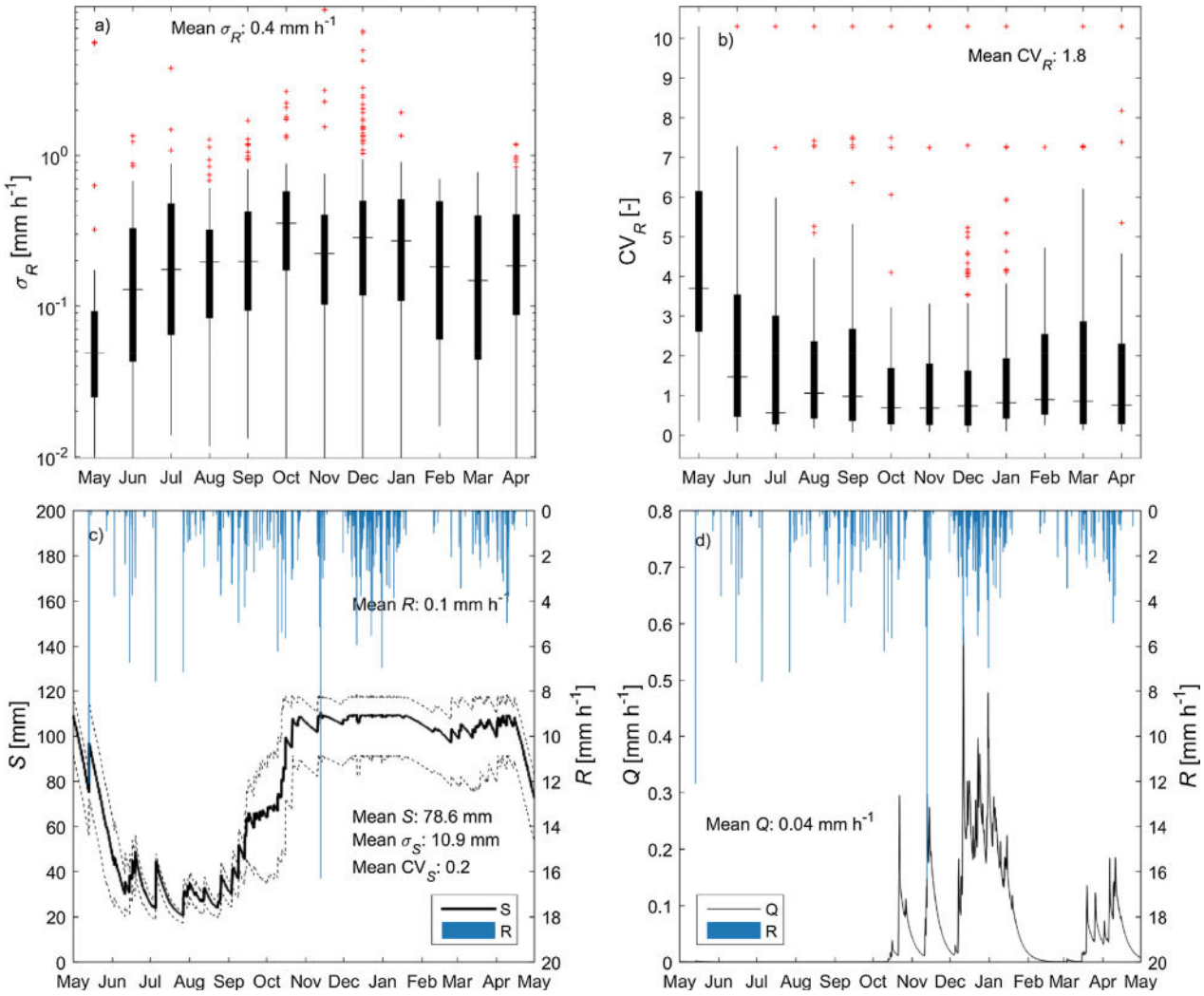

Fig. 4. Annual development of radar rainfall and its effect on the simulation of soil moisture and discharge: a) Boxplots with σ_R, and b) CV_R of radar rainfall (R). In both plots the hourly results are combined per month. c) Basin average radar rainfall and soil moisture content (S) in the rootzone. The 5th and 95th percentile for the spatial soil moisture content are represented by the dashed lines. d) Basin average radar rainfall and discharge (Q). Results are shown using the 250 m radar rainfall as input. The boxplots outer ends correspond with the 25th and 75th percentile values, and the horizontal line corresponds with the 50th percentile value. Red crosses are outliers, and correspond to values outside the ~99.3% coverage. The two lines of outliers that are visible in b) are likely due to resolution scaling. Results are based on the hydrological year May 1993 – April 1994. (For interpretation of the references to colour in this figure legend, the reader is referred to the web version of this article.)

slope of the catchment is 0.8%, while the brook itself has a mean slope of 0.2% (van der Velde et al., 2009). The brook, with a length of approx. 4 km, has 7 smaller tributaries with lengths between 300 to 1500 m (Warmerdam, 1979). The soil in this catchment consists of loamy sand with some clay, peat and gravel in the topsoil, which is situated on top of an impermeable marine clay layer of more than 20 m thick (Brauer et al., 2011). The clay layer is located at a depth that varies between 1.5 m in the southeast to 12 m in the west.

These (geo) hydrological properties are the main reason why this catchment was selected for this study: the impermeable clay layer allows for a accurately delineated watershed with almost zero flow at the boundaries. This results in a catchment with one aquifer that directly discharges to the brook, and makes it therefore very suitable for hydrological studies, which have been carried out extensively in this catchment since 1963 (Brauer et al., 2011; van der Velde et al., 2009; Rozemeijer et al., 2010; Puente et al., 1993; Hopmans and Stricker, 1989; Stricker and Brutsaert, 1978). We refer to these studies for more information about this catchment.

2.2. X-band radar

The rain data gathered for the purpose of this study was obtained from an X-band FM-CW (Frequency Modulated – Continuous Wave) Solid-State Weather Surveillance Radar, known as SOLIDAR. This radar was installed on the roof of the Electrical Engineering building of Delft University of Technology (Ligthart and Nieuwkerk, 1990), and collected data during a six-year period, from January 1991 through August 1997 (Uijlenhoet et al., 1997). Data from this radar has been used in several studies (Sassi et al., 2014; Van de Beek et al., 2010; Leijnse et al., 2008). After the processing reported by Ligthart and Nieuwkerk (1990), the range resolution of the radar data is 120 m, the angular resolution is 1.875 degrees, and the temporal resolution 16 s, which are exceptionally fine for a rainfall radar. For this study we focus on the hydrological year May 1993 through April 1994, which is the same period that was used by Van de Beek et al. (2010) and Sassi et al. (2014).

3. Methodology

3.1. Aggregation and removal of residual clutter

The radar data have been transposed to the Hupsel Brook catchment (150 km east of Delft) as if the rainfall measured by this radar would have occured over the Hupsel Brook catchment. Original radar images obtained from this radar have the typical “pizza slice” shape as shown in the left plot of Fig. 2. However, the spatially distributed model used in this study (see Section 3.4) runs at an hourly time-step and a 250 m square-grid resolution. Therefore, the original radar images had to be aggregated from a polar (120 m range resolution, 1.875-degree angular resolution, 16 s) to a rectangular grid with a 250 m spatial resolution and hourly temporal resolution. Given the i) ~3-h response time of the Hupsel Brook catchment (Brauer et al., 2016), ii) the hourly hydrological model resolution, and iii) the small number of radar rainfall pixels that can be obtained from the KNMI C-band radar (6–7 pixels vs. 106 pixels from aggregated X-band radar), the aggregation to a rectangular grid with a 250 m spatial resolution and hourly temporal resolution is a valid approach. The aggregation has been done as part of a study by Sassi et al. (2014), and an example of this is shown in Fig. 2.

Before the original radar data were aggregated, residual clutter was removed by determining a threshold for each pixel below which rainfall intensities were set to zero such that the annual rainfall of each pixel matches the lowest pixel annual rainfall (551 mm). In order to be more representative for the Hupsel Brook catchment, each pixel was subsequently scaled to match the 10-year (2000–2009) average annual rainfall over the Hupsel Brook catchment. The 10-year average annual rainfall is 801 mm according to the meteorological station located inside the catchment (Fig. 1). The scaling was achieved by multiplying the time series for each pixel with a constant factor. Hourly rainfall sums below 0.1 mm only account for 2% of the annual Hupsel Brook rainfall and are therefore classified as “drizzle” and set to zero after scaling was performed. After this step a rainfall map-series (1 May 1993–30 April 1994) for the Hupsel Brook catchment was created by extracting the gridded model outline (106 pixels, 13 rows, 16 columns; see right plot Fig. 1) from the aggregated radar rainfall images.

Table 2
Water balance with rainfall (R), discharge (Q), potential evapotranspiration (ET_p), actual evapotranspiration (ET_a), and change in storage (ΔS), as simulated by the SPHY model using radar rainfall as forcing. Water balance terms are calculated for the hydrological year May 1993 – April 1994.

Flux	mm	mm d^{-1}
R	789	2.16
Q	394	1.08
ET_p	573	1.60
ET_a	430	1.18
ΔS	−34	

3.2. Synthetic rainfall products: bootstrapping

With a synthetic rainfall product we refer to a number of virtual rain gauges randomly distributed within the Hupsel Brook catchment, where the virtual rain gauge is represented by a pixel from the radar rainfall product. The Hupsel Brook catchment consists of 106 radar pixels, which means we can construct a large number of synthetic rainfall products using 1 to 106 pixels as rain gauges. In order to determine the appropriate resolution of rainfall data to accurately describe the hydrology of this small rural lowland catchment, bootstrapping (Efron, 1979; Efron and Tibshirani, 1986) was applied to generate randomly distributed rain gauge locations for each number of

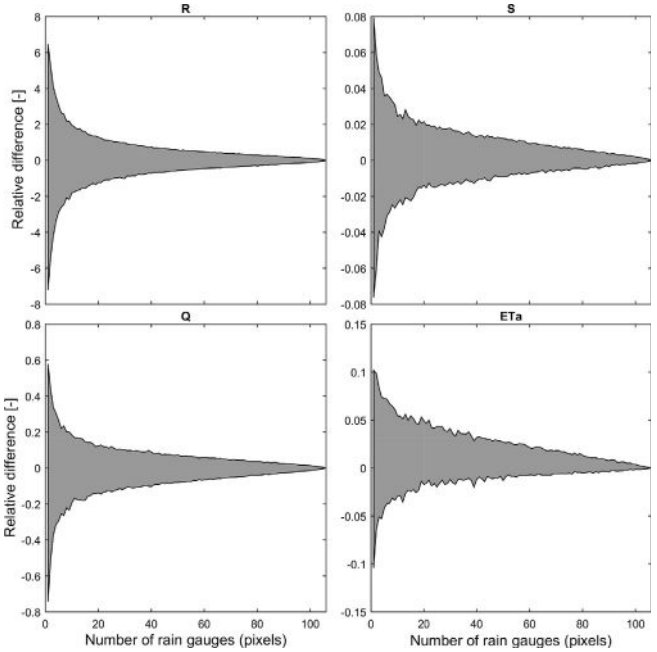

Fig. 5. 5th to 95th interpercentile range of difference between estimated basin average rainfall (R), soil moisture (S), discharge (Q), and evapotranspiration (ET_a), as function of the number of rain gauges (pixels), and the corresponding values based on radar rainfall. Differences are taken relative with respect to the average hourly value.

gauges. For this small catchment we chose the number of bootstrap samples N to be equal to the number of pixels (106). Bootstrapping was only needed for 2 to 104 rain gauges (pixels), because for 1 rain gauge and 105 rain gauges exactly 106 possibilities exist. The areal Hupsel Brook rainfall for each rainfall product is finally calculated through Inverse Distance Weighted (IDW) interpolation (Eq. (1), Shepard, 1968)) using the number of gauges involved in the random sample:

$$v_0 = \frac{\sum_{i=1}^{n} \frac{1}{d_i^p} v_i}{\sum_{i=1}^{n} \frac{1}{d_i^p}} \quad (1)$$

with v_0 the value to be estimated, n the number of points used to calculate the unknown value, v_i the known value, and d_i^p distances from data points to the point to be estimated to the power p. The default setting was used for IDW, being a power of two and an infinite search radius. This approach enables us to evaluate the uncertainty involved in estimating the areal rainfall as function of the number of rain gauges. By forcing a spatially distributed hydrological model with these synthetic rainfall products, we can evaluate the related uncertainty in the hydrological response of this catchment.

3.3. Reference evapotranspiration and initial conditions

Because hourly reference evapotranspiration (ET_r) data were not available for Rotterdam (nearest KNMI station from the X-band radar) for the hydrological year May 1993 – April 1994, we used the 10-year (2000–2009) hourly average Makkink ET_r from the meteorological station in the Hupsel Brook catchment, which is operated by KNMI. Potential evapotranspiration is then calculated for each hour by multiplying the reference evapotranspiration with a crop factor (Kc). Since the uncertainty analyses will be performed for the hydrological year May 1993 – April 1994, and soil moisture conditions are generally at field capacity at the start of the hydrological year, we chose field capacity moisture conditions as initial condition for all bootstrap runs.

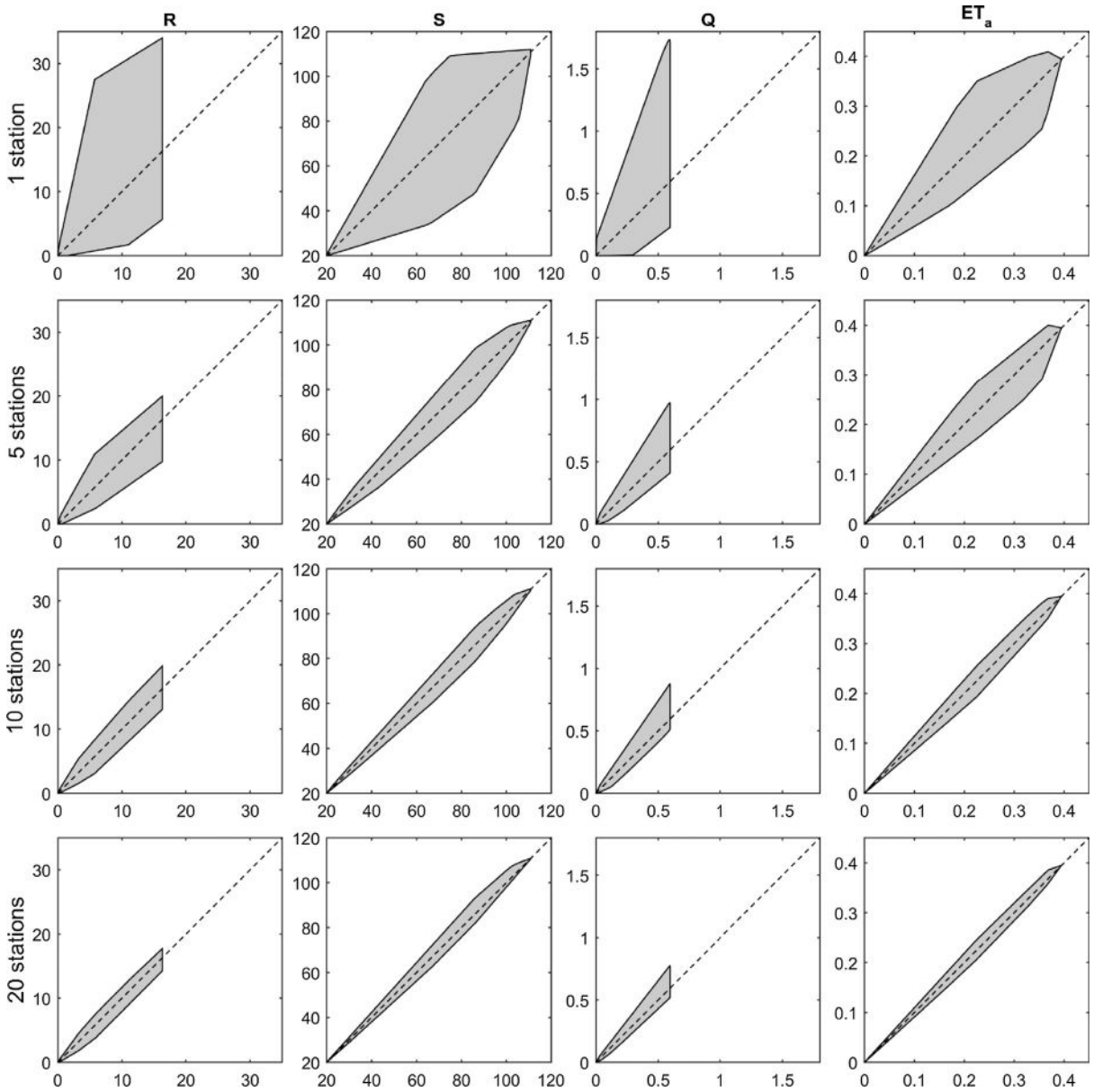

Fig. 6. From left to right: 5th to 95th interpercentile range of basin average rainfall (R), soil moisture (S), discharge (Q), and evapotranspiration (ET_a). Percentiles taken over the bootstrap samples are shown on the y-axis, while the results obtained using the original radar rainfall fields are shown on the x-axis. Results are shown from top to bottom for 1, 5, 10, and 20 stations. Units are in mm h^{-1} for R, Q, and ET_a, and in mm for S.

3.4. SPHY model set-up

3.4.1. Introduction

The simulation model used in this study is Spatial Processes in HYdrology (Terink et al., 2015), which is a spatially distributed hydrological model applied on a cell-by-cell basis. SPHY is based on the PCRaster dynamic modeling framework (Karssenberg et al., 2010; Karssenberg, 2002; Karssenberg et al., 2001) and describes the hydrological processes in a conceptual way such that changes in fluxes and storages can be evaluated over time and space. SPHY was set-up and calibrated for the Hupsel Brook catchment using the KNMI rain gauge data as input for precipitation. The gridded outline (106 pixels) of the SPHY model for the Hupsel Brook catchment is shown in the right plot of Fig. 1. For more details regarding the SPHY model we refer to Terink et al. (2015).

3.4.2. Input

As static input SPHY requires a Digital Elevation Model (DEM), land use and soil characteristics, where the latter need to be defined for the rootzone, subzone, and groundwater layer. The DEM was obtained from the AHN-2 (AHN, 2015) (Actueel Hoogtebestand Nederland, 5-m horizontal resolution) and was interpolated to the 250-m model resolution. Land use was obtained from LGN-5 (Hazeu, 2005) (Landelijk Grondgebruik Nederland). The soils in the Hupsel Brook catchment have been classified according to the PAWN-classification (Policy Analysis for the Watermanagement of the Netherlands) (Wösten et al., 1988), using the 1:50,000 soil map (v6.0) of The Netherlands. This soil map with a pixel size of 10 ha has been rasterized to the model's spatial resolution of 250 m. Except for the saturated hydraulic conductivity (K_{sat} [mm h^{-1}]), the soil physical properties required for the SPHY model were derived using pedo-transfer functions (Nemes et al., 1999). Detailed maps (5-m resolution) of the Hupsel Brook catchment, containing the saturated hydraulic conductivity and clay layer depth, were obtained from soil samples gathered throughout the years by Wösten et al. (1985). These maps contain more detail than the 1:50,000 soil map, and were therefore used to derive a 250-m resolution K_{sat} and clay depth map, using bilinear interpolation. The clay layer is almost impermeable and its depth varies between 1.5 m in the Southeast to 12 m in the West. We have assumed this layer to be completely impermeable in the model, and therefore the three soil layers in the SPHY model represent the soil properties of the Hupsel catchment untill the clay layer. Because of the shallow clay layer depth, the total thickness of the three SPHY soil layers is restricted to 1.5 m for locations where the clay layer resides 1.5 below the surface. SPHY is generally applied using a rootzone thickness of 0.4 m, meaning that 1.1 m is left for the subzone and groundwater layer. To guarantee i) the integration of the Hupsel Brook catchment's soil hydraulic properties (untill the clay layer) into the three soil layers of the SPHY model, and ii) maintain representative SPHY model soil layer depths, we need to scale the thickness of these layers for those cells where clay depth is >1.5 m. This was achieved by fixing the rootzone layer thickness at the generally applied 0.4 m, while appointing a minimum thickness of 0.9 m for the subzone and 0.2 m for the groundwater layer. For pixels where clay is >1.5 m below the surface, the layer thicknesses of the subzone and groundwater layer were scaled using the pixel's clay depth and the area's maximum and minimum clay depth. The meteorological station in the Hupsel Brook catchment (Fig. 1) provides hourly values for rainfall and ET_r, which were used to force the SPHY model for the period 2000–2009.

4. Results

The results of the model calibration are described in Section 4.1. To evaluate the impact of the limited sampling of a given number of rain gauges on the hydrological simulations of a small rural lowland catchment, we analyzed the hydrological response using radar rainfall as input (Section 4.2), and compared that simulation to those obtained using the bootstrapped rainfall fields as input. The uncertainties involved in sampling a given number of rain gauges are analyzed for two different time frames; the overall uncertainty we may experience during one year (Section 4.3), and the uncertainty during individual events (Section 4.4). The overall uncertainty focuses on basin-averaged fluxes (Section 4.3.1) as well as the spatial variability of these fluxes (Section 4.3.2).

4.1. Model calibration

With 2000 as initialization year, SPHY was calibrated using discharge measured at the outlet during the period 2001–2009. No discharge observations were available for 2004, the first 3 months of 2005, and from August 2006 through March 2007. Table 1 shows the optimized model parameters that were obtained through calibration using the Model-Independent Parameter Estimation (PEST) package

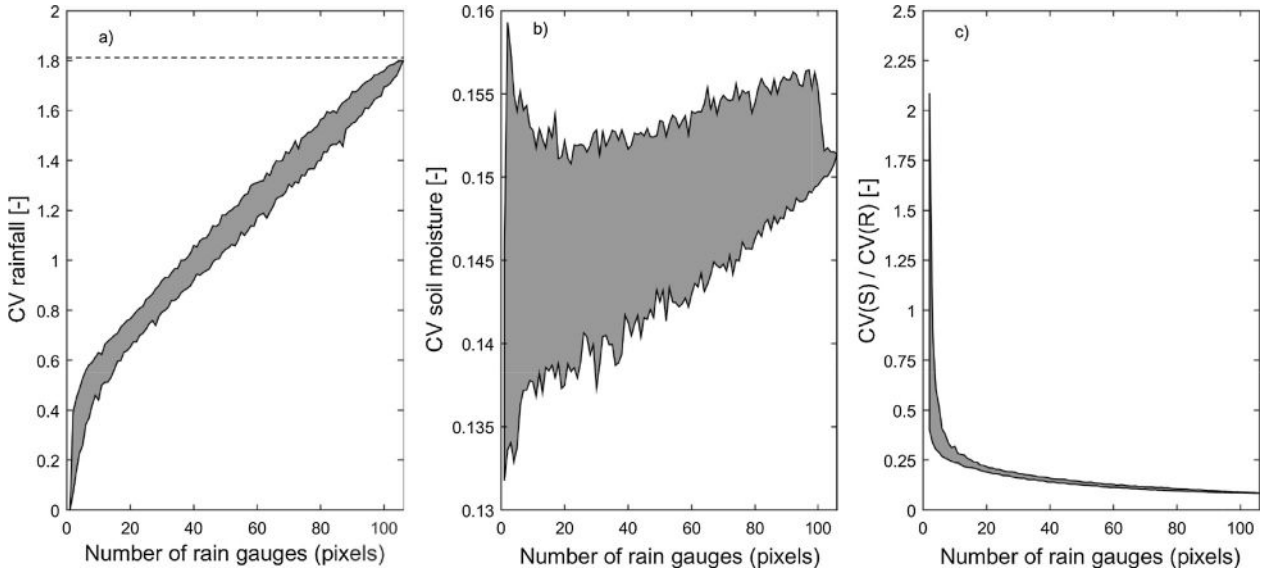

Fig. 7. 5th to 95th interpercentile range of the average hourly CV for a) rainfall, b) soil moisture, and c) the ratio between the average hourly CV of soil moisture and rainfall. Results are shown as function of the number of gauges (pixels).

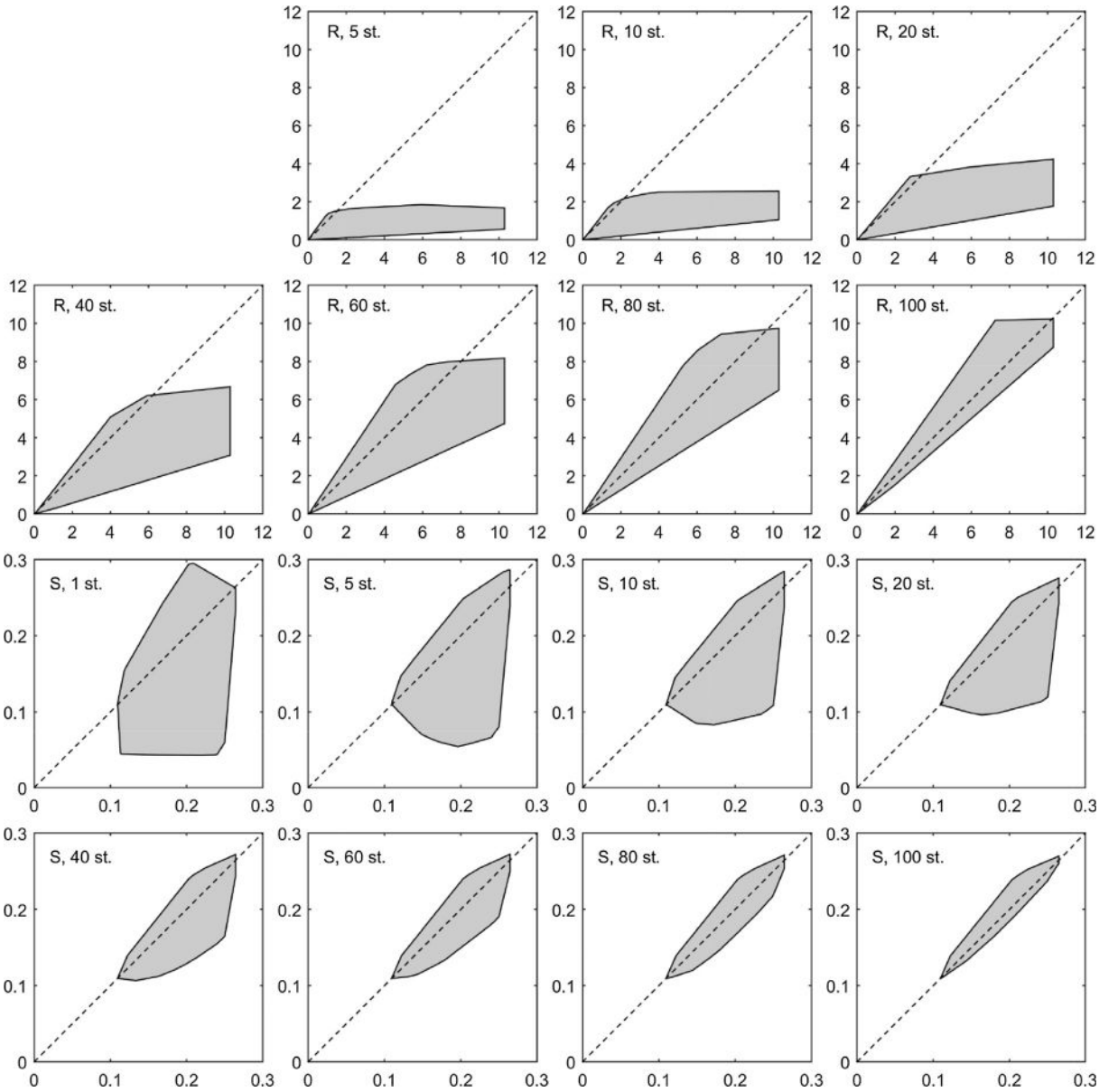

Fig. 8. 5th to 95th interpercentile range with CVs of rainfall (*R*) and soil moisture (*S*). Percentiles are taken over the number of bootstrap samples and are shown on the y-axis, while the results obtained using radar are shown on the x-axis. Results are shown for 1, 5, 10, 20, 40, 60, 80, and 100 stations, indicated as st. For rainfall there is no CV for 1 station, and is therefore not shown.

(Doherty, 2005). PEST optimizes the parameters using the Gauss-Marquardt–Levenberg (Fletcher, 1973) method for which the discrepancies between model simulations and corresponding observations are reduced to a minimum in the weighted least squares sense.

Observed vs. calibrated simulated discharge is shown in Fig. 3. For the calibration period 2001–2009 a Nash–Sutcliffe (NS) efficiency (Nash and Sutcliffe, 1970) of 0.70, Root-Mean-Squared-Error (RMSE) of 6.56 mm, and Bias of −8.7% were obtained. Strong seasonal discharge patterns can positively affect the NS because a model is generally well capable of simulating these seasonalities. Therefore, we have calculated the NS for some individual years as well. This resulted in NS-values of 0.73, 0.82, 0.69, and 0.63 for 2001, 2002, 2008, and 2009, respectively. Based on these numbers we conclude that the discharge dynamics of the calibrated model can be considered as "good" (Foglia et al., 2009). The average annual rainfall for this period is 793 mm, and SPHY simulates an average annual discharge of 287 mm, an actual evapotranspiration of 505 mm, and a change of storage of 1 mm. The negative model bias (-8.7%) indicates a slight underestimation of the average observed discharge (25 mm). Based on the performance indicators and water balance we consider the calibrated model suitable for the remainder of this study.

4.2. Hydrological response using radar rainfall

This section analyzes the hourly radar rainfall throughout the hydrological year May 1993 – April 1994, and its impact on the simulation of soil moisture and discharge. Fig. 4 shows boxplots of hourly spatial standard deviations (σ_R; top left) and spatial coefficients of variation (CV_R; top right) of the radar rainfall product (both plots show the hourly results combined per month), the simulated soil moisture content in the rootzone (bottom left), and the resulting brook discharge at the outlet (bottom right). Results are based on the hydrological year May 1993 – April 1994. Basin-average radar rainfall is shown in the bottom plots as well. Rainfall totals 789 mm over the entire year, and shows the highest intensity during November (16.3 mm h^{-1}). The spatial variability of radar rainfall, expressed as σ_R, is also highest for this event. December

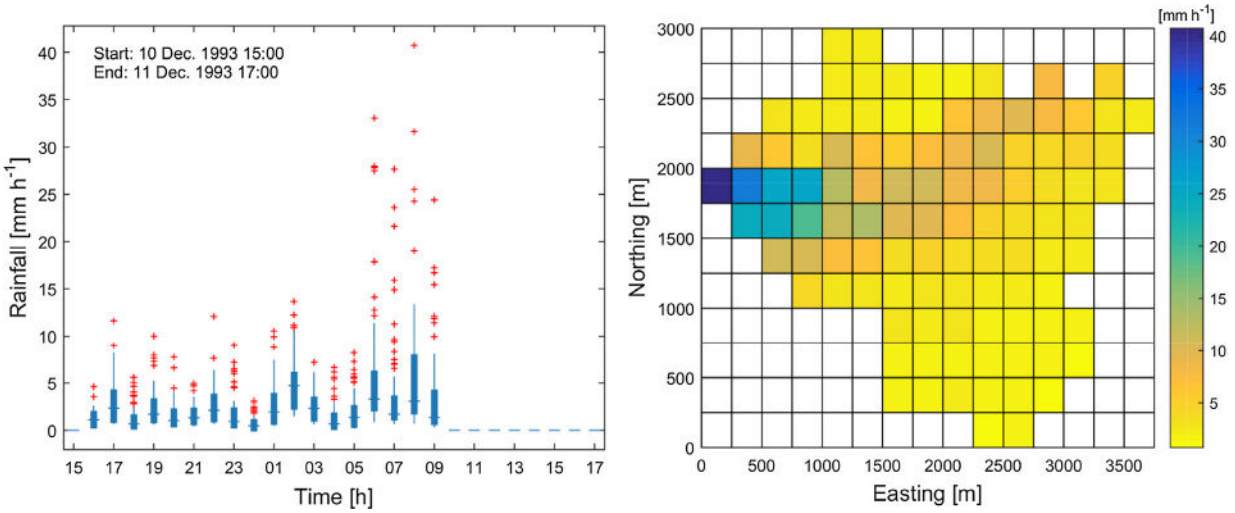

Fig. 9. Left: boxplot for the 10–11 December 1993 rainfall event, with each box representing the spatial radar rainfall distribution. The boxes outer ends correspond to the 25th and 75th percentile values, and the horizontal line corresponds to the 50th percentile value. Red crosses are outliers and correspond to values outside the ~99.3% coverage. Hours on the x-axis correspond to the end hour of each hourly time interval. Right: radar rainfall on 11 December 1993 between 7:00 and 8:00. (For interpretation of the references to colour in this figure legend, the reader is referred to the web version of this article.)

receives the largest bulk of rainfall, and is characterized as the month with the highest spatial variation in rainfall. The CV_R for this month, as well as for other winter months, are small compared to those in May–August, which is due to the larger amount of winter precipitation. May is characterized by the highest CVs, being the result of a few rainfall events with a relatively small amount of rainfall, but with high spatial variability. The large amount of rainfall, together with the high soil moisture content and low evapotranspiration, results in most discharge being generated during December 1993 and January 1994. The 5th and 95th percentiles indicate that there is substantial spatial variation in the soil moisture content, which is mainly driven by the spatial distribution of rainfall. The soil properties account for the remaining spatial variation in soil moisture content, which is more evident during summer months when there is less rain and soil moisture contents are rather low. As a result, hardly any discharge is simulated during the first 5 months. Since rootzone soil moisture contents range between 20 and 30 mm (in a rootzone of 400 mm) during summer, and SPHY reduces the amount of evapotranspiration if the soil moisture content in the rootzone drops below wilting point (pF3.0≈49 mm), we notice a relatively strong reduction in evapotranspiration (~25%). Table 2 shows the water balance as simulated by the SPHY model for the hydrological year May 1993 – April 1994.

4.3. Overall uncertainty

4.3.1. Basin averages

For each number of gauges, 106 time series of areal rainfall fields were constructed using bootstrapping and inverse distance interpolation (Section 3.2). The SPHY model was forced with these 106 × 106 rainfall fields and the resulting basin averaged fluxes are compared with those obtained using the radar rainfall as forcing. Fig. 5 expresses the uncertainty in basin average rainfall, soil moisture, discharge, and evapotranspiration as function of the number of virtual rain gauges. Uncertainty is expressed as the 5th to 95th interpercentile range of 106 bootstrap samples with 8760 hourly differences between interpolated virtual rain gauges and the radar rainfall. Differences are taken relative with respect to the "true" value averaged over the hydrological year (Table 2). Fig. 5 shows that if we use only one rain gauge to represent the areal Hupsel Brook rainfall, we may introduce an uncertainty that could be more than six times the average hourly rainfall, which compares to an uncertainty of nearly 0.54 mm h^{-1}. This means that 90% of the time, the absolute error is smaller than 0.54 mm h^{-1} for hourly rainfall accumulations if only a single rain gauge is available. Adding more rain gauges would reduce this uncertainty rapidly; with 10 rain gauges the uncertainty reduces to twice the average hourly rainfall, and more than 40 gauges are required to reduce the uncertainty to a value smaller than the average hourly rainfall.

The number of gauges used to estimate the areal rainfall of the Hupsel Brook catchment has an impact on the simulated hydrological behaviour of this small rural lowland catchment. The uncertainty associated with estimating areal rainfall has the largest effect on the simulated discharge, and to a lesser extent on the simulated soil moisture and actual evapotranspiration. The topsoil, which basically contains loamy sand, has a high saturated hydraulic conductivity (basin average 213 mm h^{-1}). As a consequence, any water surplus above field capacity leaves the soil column relatively quickly as discharge, hence the effect of erroneus areal rainfall estimation on the simulation of soil moisture content is minor in this case. One rain gauge may result in a soil moisture simulation uncertainty that is 8% of the annual average rootzone soil moisture content (~79 mm), which corresponds to ~6 mm. Although with one rain gauge the uncertainty in simulated hourly discharge will be smaller than the average hourly discharge, it may approach 60% of the average hourly discharge. This interpercentile range is reduced to ± 20% if 10 rain gauges are used. With 40 rain gauges or more the uncertainty in simulated hourly discharge becomes smaller than 10% of the average hourly discharge. For the actual evapotranspiration, there is a 90% probability that the uncertainty is within 10% of the average evapotranspiration if one rain gauge is used, which corresponds to ~0.1 mm d^{-1}.

Fig. 6 shows from top to bottom for 1, 5, 10 and 20 gauges, the values obtained using radar rainfall (i.e., the average of all 106 pixels) on the x-axis versus the 5th and 95th percentiles of the 106 bootstrap samples on the y-axis. The temporal resolution of interest is hourly. It is clear that if more rain gauges are used to estimate the areal rainfall, the simulated hydrological fluxes get closer to those simulated using the original radar rainfall fields. The near-linearity for soil moisture and actual evapotranspiration indicates that one rain gauge is sufficient to obtain a reasonably bias-free simulation of these fluxes in the Hupsel Brook catchment. With 10 rain gauges or more, the simulated values for soil moisture and actual evapotranspiration are almost identical to those simulated using radar rainfall. With one rain gauge we estimate a 95th percentile basin-average rainfall intensity of 35 mm h^{-1}, while radar indicates 17 mm h^{-1} for this paricular event. For discharge the 95th percentile is 1.7 mm h^{-1} with one rain gauge, while this is

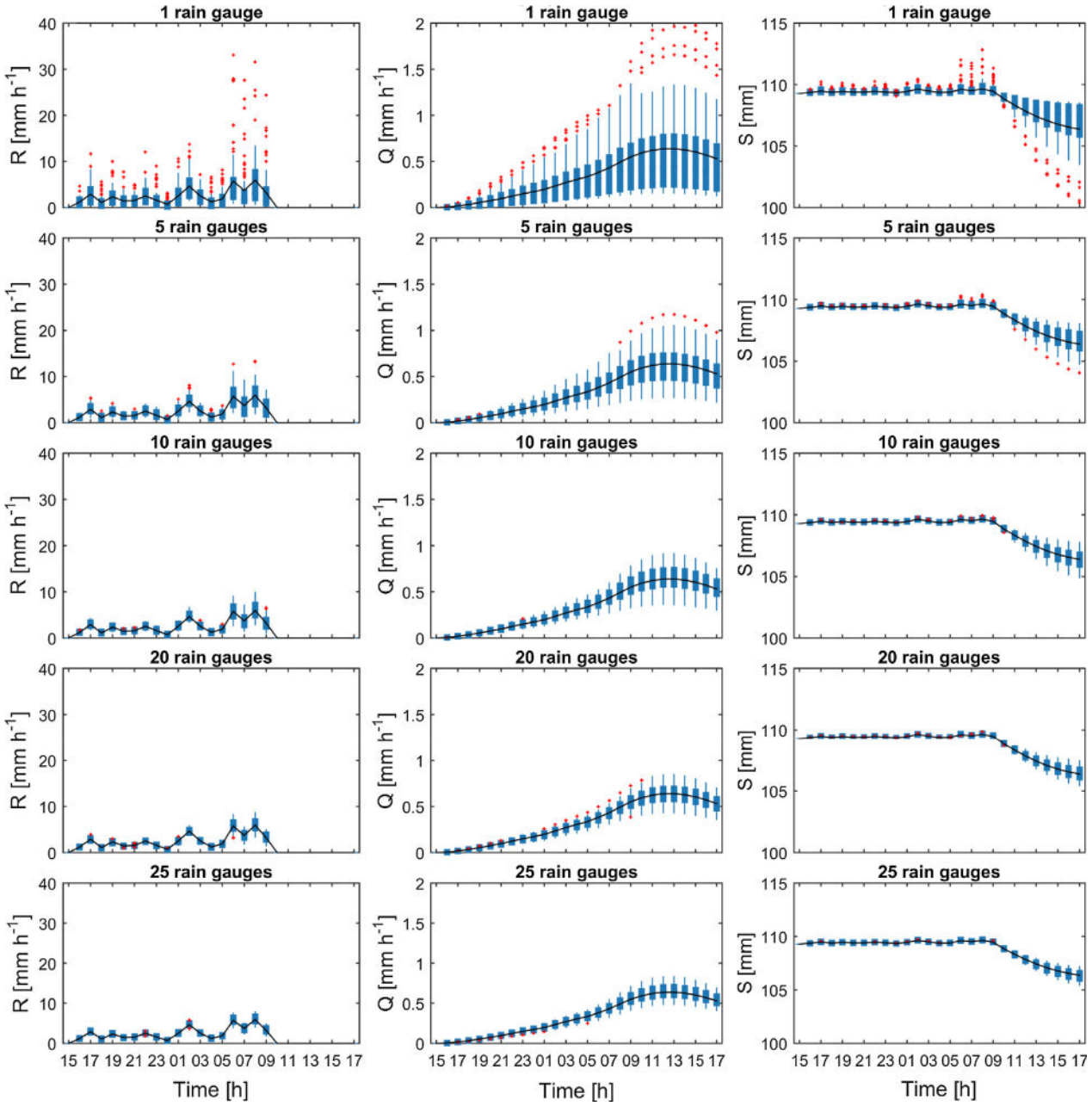

Fig. 10. Boxplots showing, as function of the number of rain gauges, the uncertainty in basin average rainfall (R), discharge (Q), and soil moisture (S) for the 10–11 December 1993 rainfall event. The boxes outer ends correspond to the 25th and 75th percentile values, and the horizontal line corresponds to the 50th percentile value. Red crosses are outliers, and correspond to values outside the ~99.3% coverage. Hours on the x-axis correspond to the end hour of each hourly time interval. The black line represents the "true" values for rainfall, discharge, and soil moisture, based on the complete radar rainfall fields. (For interpretation of the references to colour in this figure legend, the reader is referred to the web version of this article.)

0.6 mm h^{-1} if true basin-average rainfall is used as input. This is related to the fact that the distribution of hourly rainfall accumulations is extremely asymmetrical. Adding 4 rain gauges results in an appreciably reduced uncertainty of the simulated discharges. Although we may still over- or underestimate the discharge during some events, the addition of 4 gauges improves the simulation of discharge substantially. With more than 10 rain gauges we are able to have a areal rainfall estimate that is more or less equal to that calculated using radar rainfall.

4.3.2. Spatial variability

Fig. 7 shows the 5th to 95th interpercentile range of the average hourly CV for rainfall (a) and soil moisture (b). The average CV has been calculated as the average of all hourly CVs in one particular bootstrap sample. The true average hourly CV is 1.8, being substantially higher than the CV obtained using two rain gauges, which ranges between 0 and 0.4. A nearly linear increase in CV can be seen if more rain gauges are added. It is also interesting to note that it takes more rain gauges to match the spatial variability of radar rainfall, than the number of gauges required to match the basin average radar rainfall (Fig. 5).

Although the CV of rainfall increases if more rain gauges are used, this is less evident for the CV of soil moisture. The spatial distribution of soil moisture content is not only a function of rainfall, but also of soil properties, land cover, and model properties. This explains why a unique combination of a few rain gauges, soil properties and land cover may lead to a slightly higher soil moisture CV than what may be

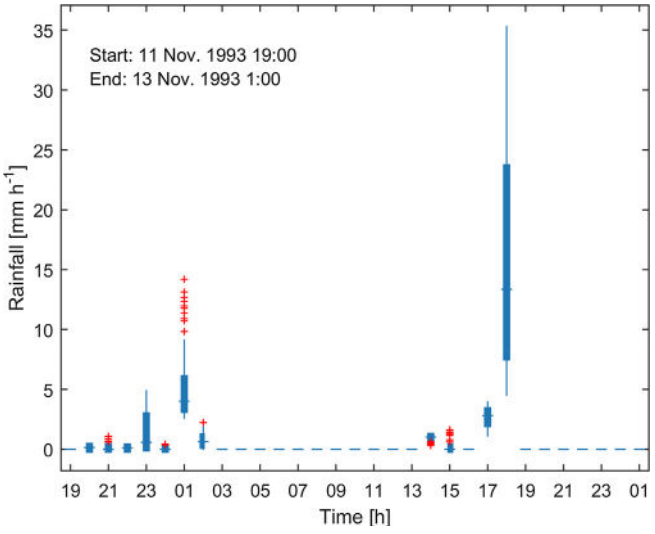

Fig. 11. Boxplot for rainfall event on 11–13 November 1993 with each box representing the spatial radar rainfall distribution. The boxes outer ends correspond to the 25th and 75th percentile values, and the horizontal line corresponds to the 50th percentile value. Red crosses are outliers, and correspond to values outside the ~99.3% coverage. Hours on the x-axis correspond to the end hour of each hourly time interval. (For interpretation of the references to colour in this figure legend, the reader is referred to the web version of this article.)

obtained by using true rainfall. If the soil moisture CV obtained using a few rain gauges is larger than the soil moisture CV obtained using radar rainfall, then the soil hydraulic properties and land cover properties have a larger contribution to the soil moisture CV than rainfall alone. However, it is clear that the bulk of the interpercentile range is below 0.151 (obtained using true rainfall), which implies that the largest contribution to the soil moisture CV comes from rainfall. To evaluate more precisely to what extent the captured spatial rainfall variability, being a function of the number of rain gauges, accounts for the spatial soil moisture distribution, and to what extent the spatial soil moisture distribution is due to the memory of the hydrological model, the average CV of soil moisture is divided by that of rainfall. We have plotted this ratio (5th and 95th percentile) as function of the number of rain gauges (Fig. 7, c). Using one rain gauge obviously results in a zero CV for rainfall and therefore results are plotted for more than two rain gauges. Based on this figure we may conclude that on average at least three rain gauges are required to add more spatial variation in the simulated soil moisture content of a small rural lowland catchment than is contributed by the model's memory (soil properties and land cover). It is clear that the number of rain gauges quickly overrules the spatial variation in soil moisture content that is contributed by the model's memory.

Fig. 8 shows the hourly CVs obtained using radar rainfall (x-axis) vs. the 5th and 95th CV percentiles of the 106 bootstrap samples (y-axis). Results are shown for 1, 5, 10, 20, 40, 60, 80, and 100 stations, and are shown for rainfall (R) and soil moisture (S). These are hourly CVs and therefore not averaged over the entire year, as was done in Fig. 7. As shown before, a substantial number of rain gauges is required to capture the same spatial variability in rainfall as obtained when using radar rainfall. More than 80 rain gauges are required to capture the spatial variability of radar rainfall. This is a substantial number of rain gauges (approx. 12 gauges km^{-2}), considering the small size of the Hupsel Brook catchment (6.5 km^2). The number of rain gauges required to match the spatial variability of radar rainfall is therefore substantially higher than the number of gauges required to match the basin average radar rainfall (Fig. 6). Using radar rainfall as input, the hourly average CV of simulated soil moisture equals 0.15 (Fig. 4). The small hourly CVs of simulated soil moisture (Fig. 8) indicate that the spatial variation in soil moisture is relatively small, which results from the high saturated hydraulic conductivity (on average 213 mm h^{-1}) that causes any water surplus above field capacity to leave the soil column relatively quickly as discharge.

4.4. Single events

Section 4.3 focused on the uncertainties in rainfall, soil moisture, discharge, and evapotranspiration that may occur within the time frame of one year as a function of the number of rain gauges used for estimating the areal rainfall. This section continues this analysis by analyzing two rainfall events in detail. For these events the SPHY model was forced using the same bootstrapped rainfall fields for the rain gauges as done in Section 4.3, assuming soil moisture is initially at field capacity.

4.4.1. 10–11 December 1993

The first event starts on the 10th of December 1993 at 15:00 (local time) and ends on the 11th of December 1993 at 09:00. The "true" radar rainfall, including the spatial rainfall distribution, is shown in Fig. 9. This event is interesting because it rains continuously with a rate of approx. 3 mm h^{-1} for 18 h, with several pixels giving significantly higher rainfall intensities. The rainfall sum for this event is approx. 35 mm for the majority of pixels, and ranges from 130 to 160 mm for a few pixels. This substantial difference in rainfall intensity between the radar pixels may be questionable. Therefore, the rainfall intensities for all radar pixels during the highest intensity rainfall hour (11 December 1993, 07:00–08:00) are shown in the right plot of Fig. 9. Since the higher rainfall pixels are clustered, as one would expect for rainfall, we conclude that the radar signal can be trusted for this event.

Fig. 10 reflects the uncertainty in basin average rainfall (R), discharge (Q), and soil moisture (S) for this event, as function of the number of rain gauges. Using the radar rainfall the discharge peaks at 13:00, which is 4 h after the last hour with rainfall, whereas the soil moisture content declines immediately after it stops raining. It is clear that the uncertainty in basin-average rainfall, discharge, and soil moisture can be signficant if only one rain gauge is used. Especially at the end of the event, where radar rainfall intensities are highest, the areal rainfall estimated using one rain gauge can vary between 0 and 35 mm h^{-1}. Compared to the radar rainfall intensity (approx. 5 mm h^{-1}), the potential error ranges between −100 and 600%. The resulting uncertainty in the simulated discharge increases until the river discharge peaks, which is 21 h after the start of the event. At this peak the reference discharge is approximately 0.6 mm h^{-1}, whereas using only one rain gauge may result in a simulated discharge of 0.2–2 mm h^{-1}, which is an uncertainty that ranges between −67 and 233%. Interestingly, the uncertainty in simulated soil moisture content, which is much smaller compared to that of discharge, starts increasing after it has stopped raining, and ranges between −6 and 2%. Adding more rain gauges to estimate the areal rainfall results in better simulations for discharge and soil moisture, with the largest positive effect on discharge. With 5 rain gauges the range of potential errors in discharge at the time of peak has dropped to between −50 and 100%. This range becomes −17 to 33% if 25 rain gauges are used.

4.4.2. 11–13 November 1993

The second selected rainfall event starts on the 11th of November 1993 at 19:00 and ends on the 13th of November 1993 at 01:00. Fig. 11 shows the "true" radar rainfall for this event, including the spatial rainfall distribution. Compared to the first event this event shows a different pattern; for a duration of 7 h we notice some initial rainfall with intensities between 0 and 9 mm h^{-1}, with a few pixels measuring 10–14 mm h^{-1} during one specific hour, followed by a period of 12 h

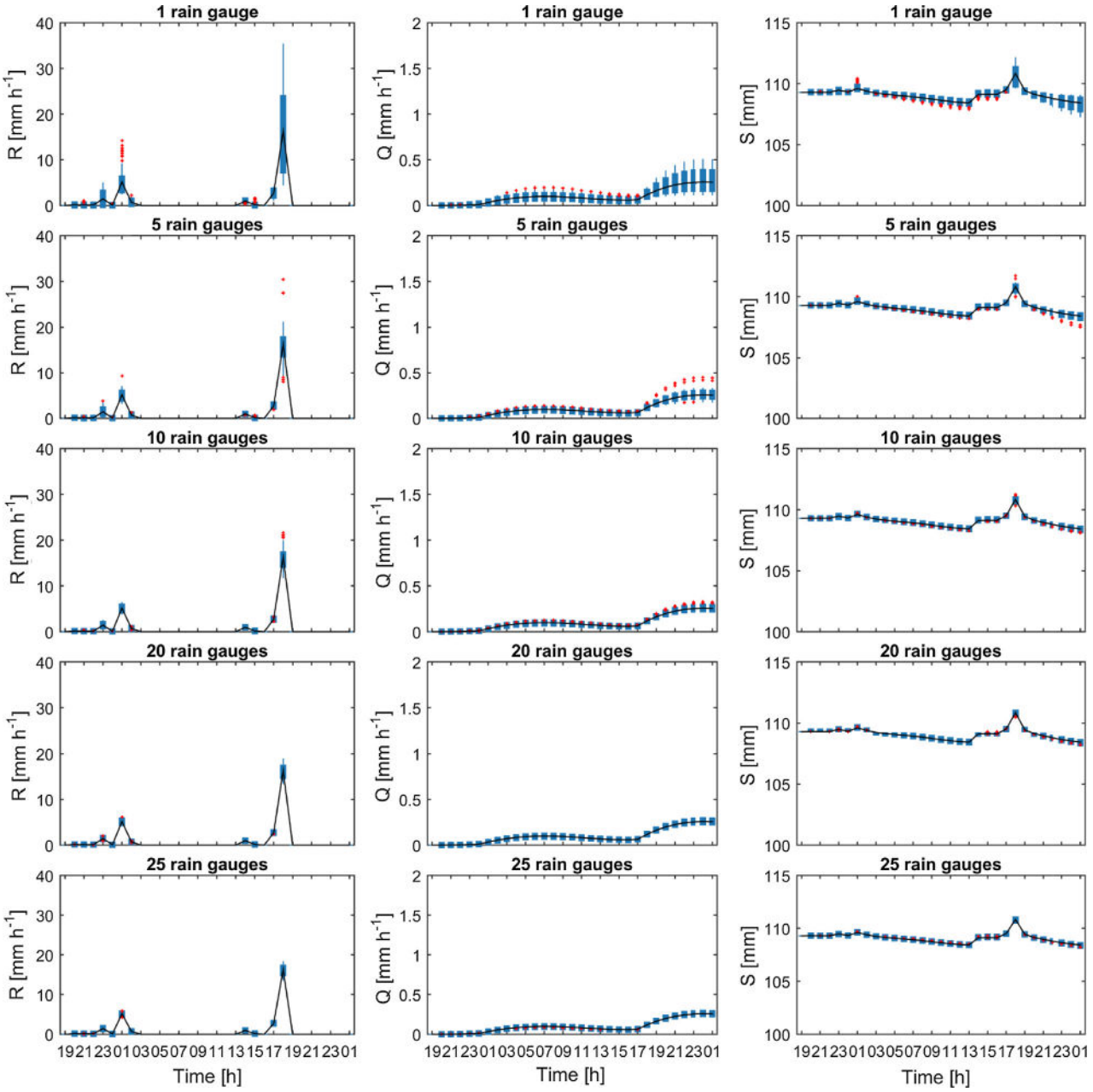

Fig. 12. Boxplots showing for 1, 5, 10, 20 and 25 rain gauges the uncertainty in basin average rainfall (R), discharge (Q), and soil moisture (S) for the 11–13 November rainfall event. The boxes outer ends correspond to the 25th and 75th percentile values, and the horizontal line corresponds to the 50th percentile value. Red crosses are outliers, and correspond to values outside the ~99.3% coverage. Hours on the x-axis correspond to the end hour of each hourly time interval. The black line represents the "true" values for rainfall, discharge, and soil moisture, based on the complete radar rainfall fields.

without rain, and finally another event ending at 18:00 with rainfall intensities of 5–35 mm h^{-1}. This day is relevant because it actually contains two different events; a bit of initial rainfall followed by a dry spell and finally a second event giving the bulk of the rainfall, being an accumulated 15–48 mm of rain.

Fig. 12 shows the uncertainty in basin average rainfall (R), discharge (Q), and soil moisture (S) for this event, as function of the number of rain gauges. We can distinguish two discharge peaks as a result of the two rainfall events. As expected we notice a recession in the soil moisture contents after the end of each rainfall event. It is clear that, although the uncertainty in basin-average rainfall is substantial for this event (−67 to 133%), the uncertainties in simulated discharge and soil moisture, using one rain gauge, are smaller compared to the 10–11 December event. This can be explained by the nature of this event, being less spatially variable (Fig. 11 vs. Fig. 9), with a lower total rainfall sum and a dry spell in between the two events. The 10–11 December event was characterized by an 18-h period of continuous rainfall with intensities between 3 and 18 mm h^{-1}, with a few pixels giving 130–160 mm h^{-1}. This resulted in a rising discharge peak with errors increasing in time as the peak grew in size, which is certainly not the case for the 11–13 November event. One rain gauge for this event results in a simulated discharge error of 0.10–0.25 mm h^{-1}, which is −40 to 100% of the reference discharge. With 5 rain gauges the error in areal rainfall ranges between −33 and 100%, while the error in simulated discharge ranges between −20 and 20%. Adding more rain gauges reduces this error less rapidly compared to that of the 10–11 December event. Errors made in the simulation of soil moisture contents are negligible for this event.

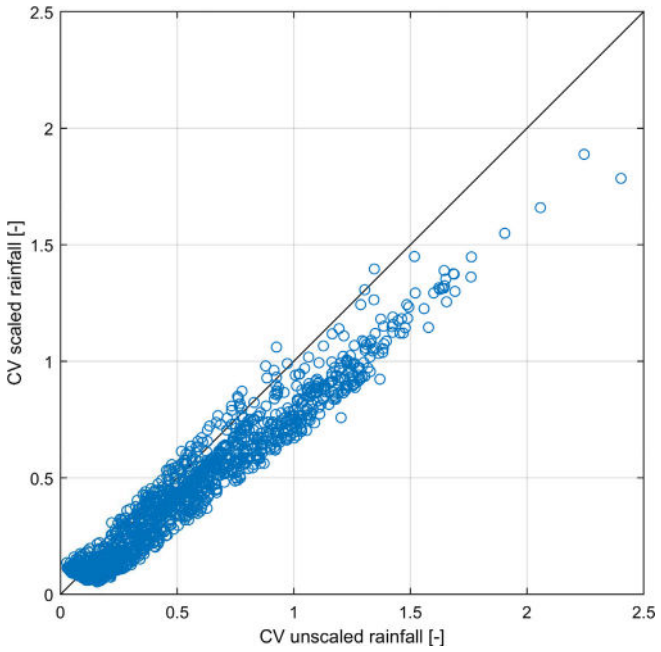

Fig. 13. Spatial CVs of hourly radar rainfall before clutter removal and scaling (x-axis) vs. spatial CVs of hourly radar rainfall after clutter removal and scaling (y-axis).

5. Discussion

It is well-known that data obtained from weather radars are affected by multiple sources of error (Hazenberg et al., 2011). This was also demonstrated by Berne et al. (2005), who found a significant underestimation of observed discharge if the lumped HBV model was forced with radar estimated rainfall. Data from the X-band radar used in the current study were not corrected for these sources of error, and may therefore be less representative for the "true" rainfall. Local errors in the radar rainfall fields, known as residual clutter, were removed using a variable threshold (Section 2.2). The unrealistically high spatial variation caused by residual clutter in the radar data was effectively removed by applying this variable threshold. A comparison between the hourly CVs of the uncorrected and corrected rainfall fields indeed shows a reduction in spatial variation (Fig. 13). Residual clutter that was not removed through this method could create additional spatial variation that would not be there in the "true" rainfall, and could therefore influence our results. However, since the synthetic rainfall products are derived from one and the same X-band radar product, the relative difference between them is not affected by the sources of error that could be present in the X-band rainfall data, and the corrections we have applied to it. Hence, we argue that this dataset is suitable to study the sensitivity of a hydrological model to the input rainfall sampling.

The areal rainfall over the Hupsel Brook catchment for each synthetic rainfall product was calculated using Inverse Distance Weighted (IDW) interpolation (Shepard, 1968). Initially, two different interpolation techniques were used to construct synthetic rainfall products

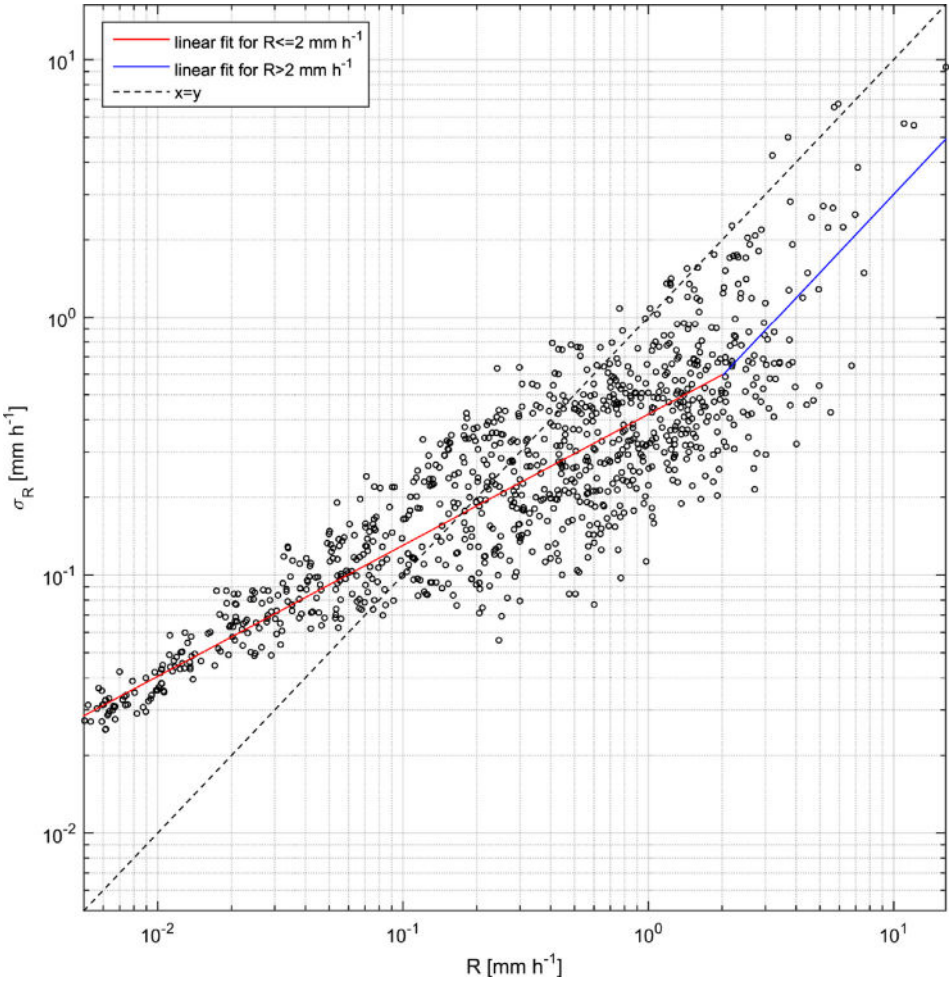

Fig. 14. Hourly standard deviations of radar rainfall pixels (σ_R) as function of the hourly basin average radar rainfall (R). Linear fits for rainfall intensities $\leqslant 2\,\mathrm{mm\,h^{-1}}$ and intensities $>2\,\mathrm{mm\,h^{-1}}$ are shown as well. Both axes are logarithmic.

from the high-resolution rainfall radar, namely simple averaging and IDW. Comparison of the resulting rainfall fields from these interpolation techniques showed hardly any difference in terms of rainfall depth or spatial variation. The selected IDW interpolation technique is a relatively "safe" interpolation technique; i.e. IDW is an exact interpolator and the maximum and minimum values can only occur at the sample points. Other interpolation techniques (e.g. Cubic Spline (Wegman and Wright, 1983)) may lead to values outside the data range, which could increase the spatial variation and thus uncertainties as well. The near linear increase in CV (Fig. 7) could be the result of the chosen interpolation method. This was further analyzed (not shown) by calculating the CV over the bootstrapped "rain gauge" pixels only; i.e. the calculated CV is independent of the interpolation method. Again, a linear increase in CV was noticed, meaning the linear increase in CV is independent of the chosen interpolation method.

The original images from the high-resolution X-band radar (120 m range resolution, 1.875-degree angular resolution, 16 s temporal resolution) were aggregated to a 250 m spatial resolution and hourly temporal resolution. Especially the temporal aggregation from 16 s to 1 h would significantly impact our results if our catchment would have been fast responding, where short-duration storm events lead to a discharge response at the outlet within the timeframe of an hour. This is particularly true for urbanized catchments (Gires et al., 2012; Ochoa-Rodriguez et al., 2015; Peleg et al., 2017). However, the Hupsel Brook catchment has a response time of three hours (Brauer et al., 2016), hence the hourly resolution is sufficient for the purpose of this study. The selected hydrological model normally runs on a 250 m spatial resolution, which is the main reason for aggregating the original 120 m range resolution to the 250 square-grid resolution. This aggregation resulted in 106 radar pixels for our study area, which is far more than what can be obtained from the operational KNMI C-band radar (6–7 pixels only).

If the X-band SOLIDAR data would have been stationed in or near the Hupsel Brook catchment, then we could have used the rain gauge located in the Hupsel Brook catchment to correct the X-band derived rainfall fields, and eventually use those corrected fields to calibrate the SPHY model. A calibrated model based on the same radar rainfall fields as used for the "true" rainfall product and synthethic rainfall products can be considered as the most optimal situation. In order to have the best possible representation of the hydrological situation of the Hupsel Brook catchment we forced the model with locally measured rainfall and evapotranspiration fields, and calibrated the model using ten years of observed discharge records, which is a similar approach to Brauer et al. (2016). In analyses of extreme precipitation over The Netherlands (Overeem et al., 2008), as well as analyses of space–time correlation structure (Van De Beek et al., 2011; Van de Beek et al., 2012), it is typically assumed that rainfall over The Netherlands can be considered statistically homogeneous. The Netherlands is a small and flat country, and climatological differences are therefore small (KNMI, 2018). The annual average rainfall in the Netherlands ranges between 700 and 900 mm (KNMI, 2018). After the removal of residual clutter, the annual rainfall for all pixels was 551 mm. Because of this climatological difference, we corrected the hourly radar rainfall fields with a constant factor to match the annual rainfall sum of Hupsel as recorded by the local rain gauge in the Hupsel Brook catchment. This is a justified approach, because i) for such a small lowland catchment one may assume that the annual rainfall sum for all radar pixels is equal (Overeem et al., 2008; Van De Beek et al., 2011; Van de Beek et al., 2012), and ii) this is not a validation study but a sensitivity analysis.

Fig. 6 (top-left plot) shows that uncertainties are larger with higher rainfall intensities. Rainfall tends to be more localized for higher intensities, thus increasing the spatial variation within the catchment. This increases the likelihood of sampling a rain pixel with more/less rainfall than what would be the case if rainfall has a lower intensity with a more uniform spatial distribution. This is also shown by Fig. 14, in which the hourly standard deviation of the radar rainfall pixels (y-axis) is plotted as function of the hourly basin average radar rainfall (x-axis). Higher rainfall intensities are associated with higher values for σ_R, and thus a higher uncertainty. The increase in σ_R is smaller compared to the increase in basin average rainfall for intensities smaller than approximately 2 mm h^{-1}. For rainfall intensities >2 mm h^{-1}, the increase in σ_R tends to be stronger, indicating an even larger uncertainty for convective systems. Other studies (e.g. Nicótina et al., 2008; Nikolopoulos et al., 2011; Ochoa-Rodriguez et al., 2015; Gires et al., 2012) found that larger catchments have a dampening effect on the rainfall variability, and thus the associated uncertainty. Although Ochoa-Rodriguez et al. (2015) and Gires et al. (2012) focused on urbanized catchments, we feel that the interplay of the catchment size with rainfall variability and the associated uncertainty in the simulation of the hydrological response needs more attention for rural lowland catchments with sizes larger than the 6.5 km^2 used in the current study.

This study revealed that areal rainfall estimations are very sensitive to the number and locations of rain gauges, which was also found by Bell et al. (2000) and Faurès et al. (1995). We found that one rain gauge may lead to an uncertainty in areal rainfall that is six times larger than the average hourly rainfall. The associated uncertainty in discharge simulations using one rain gauge is smaller, but is still 60% of the average hourly discharge, and is reduced to ± 20% if 10 rain gauges are used. Berne et al. (2005) found that the uncertainty in hourly discharge simulations associated with the sampling uncertainty of mean areal rainfall over a ~1600 km^2 catchment from 10 rain gauges was ± 25%, whereas we found an uncertainty of ± 20% if 10 rain gauges are used over a ~6.5 km^2 catchment. Their associated rain gauge density is 1 rain gauge per 160 km^2, whereas our rain gauge density is 1 rain gauge per 0.65 km^2 (i.e., much higher). Given these differences in rain gauge density, we may conclude that the uncertainty found in the current study is substantially larger than found by Berne et al. (2005). A logical explanation to this is that they forced a lumped model (HBV), whereas we maintained the spatial rainfall fields of the rainfall radar by forcing a distributed hydrological model. This increases the chance that a radar pixel with extreme rainfall coincides with a model pixel with extreme high or low conductivities, or that an extreme rainfall pixel occurs near or far away from the outlet. Additionally, we have used a very high spatial resolution X-band radar compared to the C-band radar used by Berne et al. (2005). The high spatial resolution of this X-band radar increases the chance of sampling a pixel with more extreme rainfall, and discharge simulations could thus be more uncertain. An interesting follow-up would therefore be to repeat the current study for the Hupsel Brook catchment using the lumped HBV (Lindström et al., 1997) or WALRUS (Brauer et al., 2014) model instead of the SPHY model as hydrological model. However, since these models are lumped it is not possible to evaluate soil moisture and evapotranspiration processes spatially, but only as aggregated processes over the catchment area.

The current study only analyzed the impact of different spatial rainfall resolutions on the hydrological simulations of a small lowland catchment. Peleg et al. (2013) analyzed the number of rain gauges required to adequately measure rainfall in a typical radar subpixel scale, and found that the uncertainty from averaging a number of rain stations per radar pixel decreased if timescales where increased from one minute to one day. Although the spatial resolution (1 km range resolution, 1.4-degree angular resolution) of the radar used in their study is coarser compared to the aggregated X-band radar used in our study, the effect of aggregating radar rainfall to temporal resolutions larger than one hour was not addressed in our study. Given the ~3-h response time of the Hupsel Brook catchment, time-scales smaller than one hour are less relevant to investigate, but the impact of aggregating time-scales to temporal resolutions larger than one hour is a crucial question to answer in a future study.

Although SPHY was successfully calibrated for this study, this model has some limitations that could affect the results found in this study. First, surface runoff in SPHY is only conceptualized as saturation excess runoff (Hewlettian runoff (Dunne, 1978; Hewlett, 1961)). Infiltration

excess runoff (Hortonian runoff) is not conceptualized in SPHY, which means that in the event where the rainfall intensity exceeds the infiltration capacity, the runoff in SPHY is underestimated. In other words, the uncertainty in simulated discharge, as function of the number of rain gauges, could be larger than that found in this study if rainfall intensities are high. However, since the saturated hydraulic conductivities of this specific lowland catchment are rather high, the chance that the rainfall intensity exceeds the infiltration capacity and thus that the simulated runoff underestimates the actual runoff is small. Second, the hourly model resolution of SPHY in relation to the hourly aggregated radar rainfall would be a limiting factor if the focus would be on fast responding catchments, e.g. urbanized catchments with response times in the order of minutes. For the lowland catchment used in this study, however, the hourly model resolution is not a limiting factor because the response time of the Hupsel Brook catchment is approximately 3 h (Brauer et al., 2016). Finally, streamflow routing in SPHY is conceptualized as a rather simple process where all specific cell-runoff is accumulated over the channel network and delayed with a single routing coefficient kx (Terink et al., 2015). This means that the model's flow velocity is not affected by channel properties such as slope, roughness, and wetted perimeter, which are generally implemented in more advanced routing methods that use the Manning equation (Manning, 1889) for example. Although this has not been evaluated in this study, we think that the simple routing process implemented in in SPHY has a minor effect on the simulated discharge because the Hupsel Brook is a small lowland catchment with quite uniform channel slopes. According to Warmerdam (1979), however, the presence of drains and culverts can lead to a fast discharge response if the catchment is saturated. Since culverts and drains are not conceptualized in SPHY, we feel our results are less reliable if soils are saturated and water levels in the brook are very high. An interesting follow-up study would therefore be to use a spatially distributed model with a more hydraulically based routing scheme that allows for the implementation of drains and culverts.

Other factors that may have an effect on the results presented in this study are the soil hydraulic properties and land use of the Hupsel Brook catchment. An example of this is the small uncertainty in simulated basin-average soil moisture contents and the spatial variablity thereof. This is basically due to the high saturated hydraulic conductivity of the topsoil, which causes any water surplus above field capacity to leave the soil relatively quickly as discharge, and hence the effect of erroneous rainfall estimation on the simulation of soil moisture is minor. The same holds for the simulation of evapotranspiration: due to the small amount of rainfall during pre-summer and summer, soil moisture contents are rather low (between 20 and 40 mm in a rootzone of 400 mm), which leads to a too strong reduction in evapotranspiration because SPHY reduces the amount of evapotranspiration if the soil moisture content drops below the wilting point (~49 mm). Results in our study are not affected by different intial soil moisture conditions due to the high saturated hydraulic conductivity of the topsoil in combination with the relatively low rainfall sum at the start of the hydrological year. However, the effect of different initial soil moisture conditions cannot be ignored for other basins. This was highlighted by Paschalis et al. (2014), who quantified the importance of various characteristics of the spatial and temporal structure of a rainfall event in the generation of a flood for different initial conditions of soil moisture. They found that initial soil moisture conditions and their interaction with the space–time distribution of precipitation are of paramount importance. Despite the uncertainties, we feel that the results presented in this study are representative for small (~6.5 km^2) free draining lowland catchments and soils with a high soil hydraulic conductivity.

6. Conclusions

The objective of this study was to evaluate the impact of the sampling of spatially variable rainfall by a given number of rain gauges, on hydrological simulations of a small rural lowland catchment. The most important results can be summarized as:

1. Using one rain gauge to represent the Hupsel Brook rainfall may lead to a potential error of more than six times the average hourly rainfall. More than 40 rain gauges are required to reduce this potential error to values <0.1 mm h^{-1}. The associated uncertainty in simulated discharge may approach 60% of the average hourly discharge. This is reduced to ± 20% if 10 rain gauges are used, and ± 10% if 40 rain gauges are used;
2. Because of the high saturated hydraulic conductivity of the top soil, the number of rain gauges used to represent the Hupsel brook rainfall hardly affects the simulation of soil moisture;
3. At least 12 gauges per km^2 are required to capture the spatial rainfall variation that is present in radar rainfall estimates;
4. On average, at least three rain gauges are required to add more spatial variation in the soil moisture content than is contributed by the model's memory.
5. The uncertainty in the estimation of areal rainfall and simulation of discharge is larger with higher rainfall intensities;
6. For a single rainfall event (18-h duration, average intensity of 3 mm h^{-1}) it was found that the uncertainty in peak areal rainfall estimated using one rain gauge may range between −100% (i.e., it does not rain on the gauge) and 600%. The associated uncertainty in simulated discharge for this event ranges between −67 and 233%. With 25 rain gauges the uncertainty in simulated discharge is still in the range of −17 to 33%;
7. The number of rain gauges does not affect the timing of the simulated peak discharge response, which is likely due to the high saturated hydraulic conductivity of the top soil, and the resulting short response time of the catchment.

Despite the influence of the properties of the catchment and the hydrological model on the results, we feel that the results contribute to our practical and scientific understanding of estimating areal rainfall at high spatial resolutions in order to be able to accurately describe the hydrological behaviour of small rural lowland catchments. Ideally, the approach followed in the current study should be repeated for different temporal resolutions, larger catchments, different climatological zones, and using a variety of model conceptualizations.

Acknowledgments

We like to thank Claudia Brauer from the Hydrology and Quantitative Water Management Group of Wageningen University for her expert knowledge on the Hupsel Brook catchment. This study was conducted as part of the two Daring Applications and Innovations in Sensor sYstems (DAISY) projects. DAISY 1 and DAISY 2 were financed by the EFRO programme from the Management Authority of the Dutch provinces Gelderland and Overijssel. DAISY 1 was finished in 2014, and DAISY 2 activities are carried out during the period 2017–2019. Both projects are led by the Thales Group. We therefore like to thank the Management Authority of these two provinces for financial support, and the Thales Group for succesfully leading these two projects. We also like to thank FutureWater for using their IT resources to carry out part of this work.

References

AHN, 2015. Handleiding AHN Downloaden van PDOK, Tech. Rep. Actueel Hoogtebestand Nederland (AHN), Amersfoort.

Bell, V.A., Moore, R.J., 2000. The sensitivity of catchment runoff models to rainfall data at different spatial scales. Hydrol. Earth Syst. Sci. 4 (4), 653–667. http://dx.doi.org/10.5194/hess-4-653-2000. ISSN 1607-7938, http://www.hydrol-earth-syst-sci.net/4/653/2000/.

Berndtsson, R., Niemczynowicz, J., 1988. Spatial and temporal scales in rainfall analysis –

Some aspects and future perspectives. J. Hydrol. 100 (1-3), 293–313. http://dx.doi.org/10.1016/0022-1694(88)90189-8. ISSN 00221694, http://linkinghub.elsevier.com/retrieve/pii/0022169488901898.

Berne, A., Delrieu, G., Creutin, J.-D., Obled, C., 2004. Temporal and spatial resolution of rainfall measurements required for urban hydrology. J. Hydrol. 299 (3-4), 166–179. http://dx.doi.org/10.1016/j.jhydrol.2004.08.002. ISSN 00221694, http://linkinghub.elsevier.com/retrieve/pii/S0022169404003634.

Berne, A., ten Heggeler, M., Uijlenhoet, R., Delobbe, L., Dierickx, P., de Wit, M., 2005. A preliminary investigation of radar rainfall estimation in the Ardennes region and a first hydrological application for the Ourthe catchment. Nat. Hazards Earth Syst. Sci. 5 (2), 267–274 ISSN 1684–9981, doi: 10.5194/nhess-5-267-2005, http://www.nat-hazards-earth-syst-sci.net/5/267/2005/.

Brauer, C.C., Teuling, A.J., Overeem, A., van der Velde, Y., Hazenberg, P., Warmerdam, P.M.M., Uijlenhoet, R., 2011. Anatomy of extraordinary rainfall and flash flood in a Dutch lowland catchment. Hydrol. Earth Syst. Sci. 15 (6), 1991–2005. http://dx.doi.org/10.5194/hess-15-1991-2011. ISSN 1607-7938, http://www.hydrol-earth-syst-sci.net/15/1991/2011/.

Brauer, C.C., Teuling, A.J., Torfs, P.J. F., Uijlenhoet, R., 2014. The Wageningen Lowland Runoff Simulator (WALRUS): A lumped rainfall-runoff model for catchments with shallow groundwater. Geosci. Model Dev. 7 (5), 2313–2332. http://dx.doi.org/10.5194/gmd-7-2313-2014. ISSN 19919603, http://www.geosci-model-dev.net/7/2313/2014/.

Brauer, C.C., Overeem, A., Leijnse, H., Uijlenhoet, R., 2016. The effect of differences between rainfall measurement techniques on groundwater and discharge simulations in a lowland catchment. Hydrol. Process. 30, 3885–3900. http://dx.doi.org/10.1002/hyp.10898. http://doi.wiley.com/10.1002/hyp.10898.

Doherty, J., 2005. PEST. Model-Independent Parameter Estimation. User Manual: 5th Edition, Tech. Rep., Watermark Numerical Computing.

Dunne, T., 1978. Field studies of hillslope flow processes. In: Kirkby, M.J. (Ed.), Hillslope Hydrology. John Wiley & Sons, Chichester, U.K..

Efron, B., 1979. Computers and the theory of statistics: thinking the unthinkable. SIAM Rev. 21 (4), 460–480. http://dx.doi.org/10.1137/1021092. ISSN 0036-1445, http://epubs.siam.org/doi/abs/10.1137/1021092.

Efron, B., Tibshirani, R., 1986. Bootstrap methods for standard errors, confidence intervals, and other measures of statistical accuracy. Stat. Sci. 1 (1), 54–75 http://www.jstor.org/stable/2245500.

Faurès, J.-M., Goodrich, D.C., Woolhiser, D.A., Sorooshian, S., 1995. Impact of small-scale spatial rainfall variability on runoff modeling. J. Hydrol. 173 (1-4), 309–326. http://dx.doi.org/10.1016/0022-1694(95)02704-S. ISSN 00221694, http://linkinghub.elsevier.com/retrieve/pii/002216949502704S.

Fletcher, J.E., 1973. A User's Guide to Least Squares Model Fitting, Tech. Rep. Division of Computer Research and Technology, National Institutes of Health.

Foglia, L., Hill, M.C., Mehl, S.W., Burlando, P., 2009. Sensitivity analysis, calibration, and testing of a distributed hydrological model using error-based weighting and one objective function. Water Resour. Res. 45 (6). http://dx.doi.org/10.1029/2008WR007255. n/a—n/a, ISSN 00431397, http://doi.wiley.com/10.1029/2008WR007255.

Gires, A., Onof, C., Maksimovic, C., Schertzer, D., Tchiguirinskaia, I., Simoes, N., 2012. Quantifying the impact of small scale unmeasured rainfall variability on urban runoff through multifractal downscaling: a case study. J. Hydrol. 442-443, 117–128. http://dx.doi.org/10.1016/j.jhydrol.2012.04.005. ISSN 00221694, https://www.sciencedirect.com/science/article/pii/S0022169412002685.

Hazenberg, P., Leijnse, H., Uijlenhoet, R., 2011. Radar rainfall estimation of stratiform winter precipitation in the Belgian Ardennes. Water Resour. Res. 47 (2). http://dx.doi.org/10.1029/2010WR009068. n/a—-n/a, ISSN 00431397, http://doi.wiley.com/10.1029/2010WR009068.

Hazeu, G.W., 2005. Landelijk Grondgebruiksbestand Nederland (LGN5). Vervaardiging, nauwkeurigheid en gebruik., Tech. Rep., Alterra, Wageningen.

Hewlett, J.D., 1961. Soil Moisture as a Source of Base Flow from Steep Mountain Watershed, Tech. Rep. US forest Service, Southeastern Forest Experiment Station, Asheville, North Carolina.

Hopmans, J.W., Stricker, J.N.M., 1989. Stochastic analysis of soil water regime in a watershed. J. Hydrol. 105 (1-2), 57–84. http://dx.doi.org/10.1016/0022-1694(89)90096-6. ISSN 00221694, http://linkinghub.elsevier.com/retrieve/pii/0022169489900966.

Huza, J., Teuling, A.J., Braud, I., Grazioli, J., Melsen, L.A., Nord, G., Raupach, T.H., Uijlenhoet, R., 2014. Precipitation, soil moisture and runoff variability in a small river catchment (Ardèche, France) during HyMeX Special Observation Period 1. J. Hydrol. 516, 330–342. http://dx.doi.org/10.1016/j.jhydrol.2014.01.041. ISSN 00221694, http://linkinghub.elsevier.com/retrieve/pii/S0022169414000638.

Joss, J., Waldvogel, A., 1969. Raindrop sized distribution and sampling size errors. J. Atmosph. Sci. 26 (3), 566–569. http://dx.doi.org/10.1175/1520-0469(1969)0260566:RSDASS2.0.CO;2. ISSN 0022-4928, http://journals.ametsoc.org/doi/abs/10.1175/1520-0469%281969%29026%3C0566%3ARSDASS%3E2.0.CO%3B2.

Karssenberg, D., 2002. The value of environmental modelling languages for building distributed hydrological models. Hydrol. Process. 16 (14), 2751–2766. http://dx.doi.org/10.1002/hyp.1068. ISSN 0885-6087, http://doi.wiley.com/10.1002/hyp.1068.

Karssenberg, D., Burrough, P.A., Sluiter, R., de Jong, K., 2001. The PCRaster software and course materials for teaching numerical modelling in the environmental sciences. Trans. GIS 5 (2), 99–110. http://dx.doi.org/10.1111/1467-9671.00070. ISSN 13611682, http://doi.wiley.com/10.1111/1467-9671.00070.

Karssenberg, D., Schmitz, O., Salamon, P., de Jong, K., Bierkens, M.F.P., 2010. A software framework for construction of process-based stochastic spatio-temporal models and data assimilation. Environ. Model. Software 25 (4), 489–502. http://dx.doi.org/10.1016/j.envsoft.2009.10.004. ISSN 13648152, http://linkinghub.elsevier.com/retrieve/pii/S1364815209002643.

KNMI, 2018. Regional differences in the extreme rainfall climatology in the Netherlands, https://www.knmi.nl/kennis-en-datacentrum/achtergrond/regional-differences-in-the-extreme-rainfall-climatology-in-the-netherlands.

Krajewski, W.F., Lakshmi, V., Georgakakos, K.P., Jain, S.C., 1991. A Monte Carlo Study of rainfall sampling effect on a distributed catchment model. Water Resour. Res. 27 (1), 119–128. http://dx.doi.org/10.1029/90WR01977. ISSN 00431397, http://doi.wiley.com/10.1029/90WR01977.

Lebel, T., Bastin, G., Obled, C., Creutin, J.D., 1987. On the accuracy of areal rainfall estimation: a case study. Water Resour. Res. 23 (11), 2123–2134 ISSN 00431397, doi: 10.1029/WR023i011p02123, http://doi.wiley.com/10.1029/WR023i011p02123.

Leijnse, H., Uijlenhoet, R., Stricker, J.N.M., 2007a. Hydrometeorological application of a microwave link: 2. Precipitation. Water Resour. Res. 43 (4). http://dx.doi.org/10.1029/2006WR004989. n/a—-n/a, ISSN 00431397, http://doi.wiley.com/10.1029/2006WR004989.

Leijnse, H., Uijlenhoet, R., Stricker, J.N.M., 2007b. Rainfall measurement using radio links from cellular communication networks. Water Resour. Res. 43 (3). http://dx.doi.org/10.1029/2006WR005631. n/a—-n/a, ISSN 00431397, http://doi.wiley.com/10.1029/2006WR005631.

Leijnse, H., Uijlenhoet, R., Stricker, J.N.M., 2008. Microwave link rainfall estimation: effects of link length and frequency, temporal sampling, power resolution, and wet antenna attenuation. Adv. Water Resour. 31 (11), 1481–1493. http://dx.doi.org/10.1016/j.advwatres.2008.03.004. ISSN 03091708, http://linkinghub.elsevier.com/retrieve/pii/S0309170808000535.

Ligthart, L.P., Nieuwkerk, L.R., 1990. An X-band solid-state FM-CW weather radar. Radar Signal Process., IEE Proc. F 137 (6), 418–426.

Lindström, G., Johansson, B., Persson, M., Gardelin, M., Bergström, S., 1997. Development and test of the distributed HBV-96 hydrological model. J. Hydrol. 201 (1-4), 272–288. http://dx.doi.org/10.1016/S0022-1694(97)00041-3. ISSN 00221694, http://linkinghub.elsevier.com/retrieve/pii/S0022169497000413.

Lobligeois, F., Andréassian, V., Perrin, C., Tabary, P., Loumagne, C., 2014. When does higher spatial resolution rainfall information improve streamflow simulation? An evaluation using 3620 flood events. Hydrol. Earth Syst. Sci. 18 (2), 575–594. http://dx.doi.org/10.5194/hess-18-575-2014. ISSN 1607-7938, http://www.hydrol-earth-syst-sci.net/18/575/2014/.

Manning, R., 1889. On the flow of water in open channels and pipes. Trans. Inst. Civ. Eng. Ireland 20, 161–207.

Marani, M., 2005. Non-power-law-scale properties of rainfall in space and time. Water Resour. Res. 41 (8) n/a—-n/a, ISSN 00431397, doi: 10.1029/2004WR003822, http://doi.wiley.com/10.1029/2004WR003822.

Nash, J.E., Sutcliffe, J.V., 1970. River flow forecasting through conceptual models. Part I – A discussion of principles. J. Hydrol. 10 (3), 282–290. http://dx.doi.org/10.1016/0022-1694(70)90255-6. ISSN 00221694, http://linkinghub.elsevier.com/retrieve/pii/0022169470902556.

Nemes, A., Wösten, J.H.M., Lilly, A., Oude Voshaar, J.H., 1999. Evaluation of different procedures to interpolate particle-size distributions to achieve compatibility within soil databases. Geoderma 90 (3-4), 187–202. http://dx.doi.org/10.1016/S0016-7061(99)00014-2. ISSN 00167061, http://linkinghub.elsevier.com/retrieve/pii/S0016706199000142.

Nerini, D., Besic, N., Sideris, I., Germann, U., Foresti, L., 2017. A non-stationary stochastic ensemble generator for radar rainfall fields based on the short-space Fourier transform. Hydrol. Earth Syst. Sci. 21 (6), 2777–2797 ISSN 16077938, doi: 10.5194/hess-21-2777-2017, https://search.proquest.com/openview/5ec1da896-be906f739fb2153ecc6693a/1?pq-origsite=gscholar&cbl=105724.

Nicótina, L., Alessi Celegon, E., Rinaldo, A., Marani, M., 2008. On the impact of rainfall patterns on the hydrologic response. Water Resour. Res. 44 (12) n/a—-n/a, ISSN 00431397, doi: 10.1029/2007WR006654, http://doi.wiley.com/10.1029/2007WR006654.

Nikolopoulos, E.I., Anagnostou, E.N., Borga, M., Vivoni, E.R., Papadopoulos, A., 2011. Sensitivity of a mountain basin flash flood to initial wetness condition and rainfall variability. J. Hydrol. 402 (3–4), 165–178. http://dx.doi.org/10.1016/j.jhydrol.2010.12.020. ISSN 00221694, https://www.sciencedirect.com/science/article/pii/S0022169410007857.

Ochoa-Rodriguez, S., Wang, L.P., Gires, A., Pina, R.D., Reinoso-Rondinel, R., Bruni, G., Ichiba, A., Gaitan, S., Cristiano, E., Van Assel, J., Kroll, S., Murlà-Tuyls, D., Tisserand, B., Schertzer, D., Tchiguirinskaia, I., Onof, C., Willems, P., Ten Veldhuis, M.C., 2015. Impact of spatial and temporal resolution of rainfall inputs on urban hydrodynamic modelling outputs: a multi-catchment investigation. J. Hydrol. 531, 389–407. http://dx.doi.org/10.1016/j.jhydrol.2015.05.035. ISSN 00221694 https://www.sciencedirect.com/science/article/pii/S0022169415003856.

Ogden, F.L., Sharif, H.O., Senarath, S.U.S., Smith, J.A., Baeck, M.L., Richardson, J.R., 2000. Hydrologic analysis of the Fort Collins, Colorado, flash flood of 1997. J. Hydrol. 228 (1-2), 82–100. http://dx.doi.org/10.1016/S0022-1694(00)00146-3. ISSN 00221694, http://linkinghub.elsevier.com/retrieve/pii/S0022169400001463.

Overeem, A., Buishand, A., Holleman, I., 2008. Rainfall depth-duration-frequency curves and their uncertainties. J. Hydrol. 348 (1-2), 124–134. http://dx.doi.org/10.1016/j.jhydrol.2007.09.044. ISSN 00221694, https://www.sciencedirect.com/science/article/pii/S0022169407005513.

Overeem, A., Buishand, T.A., Holleman, I., 2009. Extreme rainfall analysis and estimation of depth-duration-frequency curves using weather radar. Water Resour. Res. 45 (10). http://dx.doi.org/10.1029/2009WR007869. ISSN 00431397, http://doi.wiley.com/10.1029/2009WR007869.

Overeem, A., Leijnse, H., Uijlenhoet, R., 2013. Country-wide rainfall maps from cellular communication networks. Proc. Nat. Acad. Sci. 110 (8), 2741–2745. http://dx.doi.org/10.1073/pnas.1217961110. ISSN 0027-8424, http://www.pnas.org/cgi/doi/10.1073/pnas.1217961110.

Pardo-Igúzquiza, E., 1998. Optimal selection of number and location of rainfall gauges for

areal rainfall estimation using geostatistics and simulated annealing. J. Hydrol. 210 (1-4), 206–220. http://dx.doi.org/10.1016/S0022-1694(98)00188-7. ISSN 00221694, https://pdfs.semanticscholar.org/7d4d/069663de47e11fd769bb267b375bce6d5f31.pdf.

Paschalis, A., Molnar, P., Fatichi, S., Burlando, P., 2013. A stochastic model for high-resolution space-time precipitation simulation. Water Resour. Res. 49 (12), 8400–8417 ISSN 00431397, doi: 10.1002/2013WR014437, http://doi.wiley.com/10.1002/2013WR014437.

Paschalis, A., Fatichi, S., Molnar, P., Rimkus, S., Burlando, P., 2014. On the effects of small scale space-time variability of rainfall on basin flood response. J. Hydrol. 514, 313–327. http://dx.doi.org/10.1016/j.jhydrol.2014.04.014. ISSN 00221694, https://www.sciencedirect.com/science/article/pii/S0022169414002881.

Peleg, N., Ben-Asher, M., Morin, E., 2013. Radar subpixel-scale rainfall variability and uncertainty: lessons learned from observations of a dense rain-gauge network. Hydrol. Earth Syst. Sci 17, 2195–2208. http://dx.doi.org/10.5194/hess-17-2195-2013. www.hydrol-earth-syst-sci.net/17/2195/2013/.

Peleg, N., Fatichi, S., Paschalis, A., Molnar, P., Burlando, P., 2017. An advanced stochastic weather generator for simulating 2-D high-resolution climate variables. J. Adv. Model. Earth Syst. 9 (3), 1595–1627 ISSN 19422466, doi: 10.1002/2016MS000854, http://doi.wiley.com/10.1002/2016MS000854.

Peleg, N., Blumensaat, F., Molnar, P., Fatichi, S., Burlando, P., 2017. Partitioning the impacts of spatial and climatological rainfall variability in urban drainage modeling. Hydrol. Earth Syst. Sci 21, 1559–1572. http://dx.doi.org/10.5194/hess-21-1559-2017. www.hydrol-earth-syst-sci.net/21/1559/2017/.

Puente, C.E., Bierkens, M.F.P., Diaz-Granados, M.A., Dik, P.E., López, M.M., 1993. Practical use of analytically derived runoff models based on rainfall point processes. Water Resour. Res. 29 (10), 3551–3560. http://dx.doi.org/10.1029/93WR01294. ISSN 00431397, http://doi.wiley.com/10.1029/93WR01294.

Rabiei, E., Haberlandt, U., 2015. Applying bias correction for merging rain gauge and radar data. J. Hydrol. 522, 544–557. http://dx.doi.org/10.1016/j.jhydrol.2015.01.020. ISSN 00221694, http://linkinghub.elsevier.com/retrieve/pii/S0022169415000372.

Rafieeinasab, A., Norouzi, A., Kim, S., Habibi, H., Nazari, B., Seo, D.J., Lee, H., Cosgrove, B., Cui, Z., 2015. Toward high-resolution flash flood prediction in large urban areas – Analysis of sensitivity to spatiotemporal resolution of rainfall input and hydrologic modeling. J. Hydrol. 531, 370–388. http://dx.doi.org/10.1016/j.jhydrol.2015.08.045. ISSN 00221694, https://www.sciencedirect.com/science/article/pii/S0022169415006605.

Rozemeijer, J.C., van der Velde, Y., van Geer, F.C., Bierkens, M.F.P., Broers, H.P., 2010. Direct measurements of the tile drain and groundwater flow route contributions to surface water contamination: from field-scale concentration patterns in groundwater to catchment-scale surface water quality. Environ. Pollut. 158 (12), 3571–3579. http://dx.doi.org/10.1016/j.envpol.2010.08.014. ISSN 02697491, http://linkinghub.elsevier.com/retrieve/pii/S0269749110003672.

Sassi, M.G., Leijnse, H., Uijlenhoet, R., 2014. Sensitivity of power functions to aggregation: bias and uncertainty in radar rainfall retrieval. Water Resour. Res. 50 (10), 8050–8065. http://dx.doi.org/10.1002/2013WR015109. ISSN 00431397, http://doi.wiley.com/10.1002/2013WR015109.

Shepard, D., 1968. A two-dimensional interpolation function for irregularly-spaced data. In: Proceedings of the 1968 23rd ACM national conference, ACM Press, New York, New York, USA, pp. 517–524, ISBN 1-59593-161-9. doi: 10.1145/800186.810616, http://portal.acm.org/citation.cfm?doid=800186.810616.

Sohn, B.J., Han, H.-J., Seo, E.-K., 2010. Validation of satellite-based high-resolution rainfall products over the Korean Peninsula using data from a dense rain gauge network. J. Appl. Meteorol. Climatol. 49 (4), 701–714 ISSN 1558-8424, doi: 10.1175/2009JAMC2266.1, http://journals.ametsoc.org/doi/abs/10.1175/2009JAMC2266.1.

Stricker, H., Brutsaert, W., 1978. Actual evapotranspiration over a summer period in the Hupsel catchment. J. Hydrol. 39 (1-2), 139–157. http://dx.doi.org/10.1016/0022-1694(78)90119-1. ISSN 00221694, http://linkinghub.elsevier.com/retrieve/pii/0022169478901191.

Terink, W., Lutz, A.F., Simons, G.W.H., Immerzeel, W.W., Droogers, P., 2015. SPHY v2.0: Spatial Processes in HYdrology. Geosci. Model Dev. 8 (7), 2009–2034. http://dx.doi.org/10.5194/gmd-8-2009-2015. ISSN 1991-9603, http://www.geosci-model-dev.net/8/2009/2015/.

Uijlenhoet, R., Stricker, J.N.M., Russchenberg, H.W.J., 1997. Application of X- and S-band radars for rain rate estimation over an urban area. Phys. Chem. Earth 22 (3-4), 259–264. http://dx.doi.org/10.1016/S0079-1946(97)00141-9. ISSN 00791946, http://linkinghub.elsevier.com/retrieve/pii/S0079194697001419.

Van de Beek, C.Z., Leijnse, H., Stricker, J.N.M., Uijlenhoet, R., Russchenberg, H.W.J., 2010. Performance of high-resolution X-band radar for rainfall measurement in The Netherlands. Hydrol. Earth Syst. Sci. 14 (2), 205–221 ISSN 1607-7938, doi: 10.5194/hess-14-205-2010, http://www.hydrol-earth-syst-sci.net/14/205/2010/.

Van De Beek, C.Z., Leijnse, H., Torfs, P.J., Uijlenhoet, R., 2011. Climatology of daily rainfall semi-variance in the Netherlands. Hydrol. Earth Syst. Sci. 15 (1), 171–183. http://dx.doi.org/10.5194/hess-15-171-2011. ISSN 10275606, www.hydrol-earth-syst-sci-discuss.net/7/2085/2010/.

Van de Beek, C.Z., Leijnse, H., Torfs, P., Uijlenhoet, R., 2012. Seasonal semi-variance of Dutch rainfall at hourly to daily scales. Adv. Water Resour. 45, 76–85 ISSN 03091708, doi: 10.1016/j.advwatres.2012.03.023, http://linkinghub.elsevier.com/retrieve/pii/S0309170812000784.

van der Velde, Y., de Rooij, G.H., Torfs, P.J.J.F., 2009. Catchment-scale non-linear groundwater-surface water interactions in densely drained lowland catchments. Hydrol. Earth Syst. Sci. 13 (10), 1867–1885. http://dx.doi.org/10.5194/hess-13-1867-2009. ISSN 1607-7938, http://www.hydrol-earth-syst-sci.net/13/1867/2009/.

Villarini, G., Krajewski, W.F., 2010. Review of the different sources of uncertainty in single polarization radar-based estimates of rainfall, doi: 10.1007/s10712-009-9079-x, URL http://link.springer.com/10.1007/s10712-009-9079-x.

Villarini, G., Mandapaka, P.V., Krajewski, W.F., Moore, R.J., 2008. Rainfall and sampling uncertainties: a rain gauge perspective. J. Geophys. Res. Atmosp. 113 (11) D11102, ISSN 01480227, doi: 10.1029/2007JD009214, http://doi.wiley.com/10.1029/2007JD009214.

Warmerdam, P.M.M., 1979. Hydrological Effects of Drainage Improvement in the Hupselse Beek Catchment Area in the Netherlands, Tech. Rep. Department of Hydraulics and Catchment Hydrology, Agricultural University, Wageningen, The Netherlands.

Wegman, E.J., Wright, I.W., 1983. Splines in statistics. J. Am. Stat. Assoc. 78 (382), 351–365. http://dx.doi.org/10.1080/01621459.1983.10477977. ISSN 1537274X, http://www.jstor.org/stable/2288640?origin=crossref.

Wilson, C.B., Valdes, J.B., Rodriguez-Iturbe, I., 1979. On the influence of the spatial distribution of rainfall on storm runoff. Water Resour. Res. 15 (2), 321–328. http://dx.doi.org/10.1029/WR015i002p00321. ISSN 00431397, http://doi.wiley.com/10.1029/WR015i002p00321.

Wösten, J.H.M., Bouma, J., Stoffelsen, G.H., 1985. Use of soil survey data for regional soil water simulation models. Soil Sci. Soc. Am. J. 49 (5), 1238. http://dx.doi.org/10.2136/sssaj1985.03615995004900050033x. ISSN 0361-5995, https://www.soils.org/publications/sssaj/abstracts/49/5/SS0490051238.

Wösten, J.H.M., De Vries, F., Denneboom, J., Van Holst, A.F., 1998. Generalisatie en bodemfysische vertaling van de Bodemkaart van Nederland, 1:250.000, ten behoeve van de Pawnstudie., Tech. Rep., Stiboka.

Yang, L., Smith, J.A., Baeck, M.L., Zhang, Y., 2016. Flash flooding in small urban watersheds: Storm event hydrologic response. Water Resour. Res. 52 (6), 4571–4589. http://dx.doi.org/10.1002/2015WR018326. ISSN 19447973, https://agupubs.onlinelibrary.wiley.com/doi/full/10.1002/2015WR018326.